

SUPERSEDES NASA TM-80181, ISSUED JANUARY 1980

N 82-21603

C S C L 20 K

Unclas
09380



November 1981

Langley Research Center
Hampton, Virginia 23665

CONTENTS

	Page
SUMMARY	1
INTRODUCTION.	1
SYMBOLS	2
DESCRIPTION OF GENERAL APPROACH USED IN AND CAPABILITY OF PASCO COMPUTER CODE.	6
Overview	6
Approach and Capability.	9
Design conditions	10
Analysis.	10
Panel configuration and material.	10
Sizing, sizing variables, and constraints	11
STRUCTURAL ANALYSIS	12
Prebuckling Stress Analysis.	12
Elastic relations	12
Uniform longitudinal strain	16
Bending loads	17
Shear stress.	24
VIPASA Buckling Analysis	26
Elastic relations	27
Buckling displacements and boundary conditions.	29
Orthotropic panels with no shear loading.	30
Anisotropic panels and/or panels with a shear loading.	31
Example	33
FACTOR and F	37
Smeared Orthotropic Stiffnesses.	40
Adjusted Analysis for Shear Buckling	43
Rationale for adjusted analysis approach.	43
Calculation of adjusted buckling load	45
Example	48
SIZING.	50
Problem Statement.	50
Sizing Variables	51
Objective Function	51
Constraints.	52
Buckling or vibration	52
Material strength	53
Stiffness	54

CONTENTS - Concluded

	Page
Approximate Analysis	55
Analysis module	55
Taylor series module.	55
Sizing module	56
Sizing strategy	56
Move limits	58
Identifying critical buckling and frequency constraints.	58
Identifying other critical constraints.	60
Calculation of Derivatives of Buckling Loads	60
Multiple Load Conditions	64
Sizing Example	65
CONCLUDING REMARKS.	68
REFERENCES.	69

PASCO: STRUCTURAL PANEL ANALYSIS AND SIZING
CODE , CAPABILITY AND ANALYTICAL FOUNDATIONS

W. Jefferson Stroud and Melvin S. Anderson

SUMMARY

A computer code denoted PASCO which can be used for analyzing and sizing uniaxially-stiffened composite panels is described. Buckling and vibration analyses are carried out with a linked-plate analysis computer code denoted VIPASA, which is incorporated in PASCO. Sizing is based on nonlinear mathematical programming techniques and employs a computer code denoted CONMIN, also incorporated in PASCO. Design requirements considered are initial buckling, material strength, stiffness, and vibration frequency. The report describes the capability of the PASCO computer code and the approach used in the structural analysis and sizing.

INTRODUCTION

Stiffened panels made of metal and/or composite materials have wide application in aerospace structures. These panels are generally designed to have low mass and must meet numerous design requirements involving, for example, buckling, stiffness, material strength, and limitations on panel geometry. In an effort to increase the structural efficiency of these panels, design concepts are being explored which exhibit complex buckling modes, requiring sophisticated stability analyses. In

addition, composite panels may require relatively sophisticated stress analyses.

To address these needs, a computer code denoted PASCO has been developed for analyzing and sizing stiffened composite panels. The code attempts to balance the user requirements of generality, simplicity, rigor, and modest computer resources. This report describes the analytical foundations of PASCO to the extent that it would help a user understand the analysis and sizing procedures, select appropriate options, and interpret answers. Complex theoretical discussions are treated in the references. The users manual for PASCO, reference 1, includes an explanation of structural modeling for PASCO, a discussion of program input and output, and several illustrative examples. Design studies carried out with PASCO are described in references 2 and 3. Previous work dealing with the analysis and sizing of stiffened composite panels is discussed in references 4 and 5.

The present report begins with a discussion of the program capability and approach. There follows a discussion of the stress and buckling analyses. Finally, the structural sizing strategy is discussed.

SYMBOLS

Values are given in both SI and U.S. Customary Units. The calculations were made in U.S. Customary Units. In many cases, the FORTRAN name of the variables used in PASCO is included in the definition.

A	panel planform area shown in figure 25
\bar{A}	for closed section stiffeners, area enclosed by the closed section in one period
\bar{A}_i	$A_{11} - (A_{12})^2/A_{22}$ for plate element i
A_{jk}	laminate inplane stiffnesses and smeared orthotropic inplane stiffness defined by equation (1)
A_{jk_i}	value of laminate inplane stiffness A_{jk} for plate element i
AllL, AllU A33L, A33U	lower and upper bounds on smeared orthotropic stiffnesses A_{11} and A_{33}
ALLOW	allowables used in the material strength criteria
b	plate element width
b_i	width of plate element i
b_s	width of one period of the stiffened panel (see figs. 6 and 8)
C_i	quantities defined by equation (18)
C_{jT}	quantities associated with temperature, defined in equations (1) and (5)
CLAM(λ)	parameter used during sizing for prescribing margin of safety on buckling load with half-wavelength λ equal to L/m , defined in equation (47)
CONV1, CONV2	convergence criteria for eigenvalue analysis
D_{jk}	laminate bending stiffnesses and smeared orthotropic bending stiffnesses defined by equation (35)
D_{jk_i}	value of laminate bending stiffness D_{jk} for plate element i
D11L, D11U	lower and upper bounds on smeared orthotropic bending stiffness D_{11}
DVMOV	parameters used to determine move limits during sizing, defined in equations (54) and (55)
e, ECC	bow at panel midlength

E_1 , E1	Young's modulus of composite material in fiber direction
E_2 , E2	Young's modulus of composite material in direction transverse to fiber direction
E_{12} , E12	Shear modulus of composite material in material coordinate system
f, FREQ	frequency
F, FACTOR	scale factor that relates the input or design load to the load that causes buckling or vibration, defined in equation (39)
$F(y)$	buckling displacement function, defined in equation (36)
$f_1(y)$, $f_2(y)$	real and imaginary parts of $F(y)$, defined in equation (37)
F_1 , F_2 , F_{11} , F_{12} , F_{22} , F_{66}	functions that appear in Tsai-W. material strength criterion (see eq. (49))
G	behavioral constraint (see eq. (46))
GRANGE	constraint deletion parameter
ITHERM	parameter used to indicate the manner in which a bending moment produced by temperature or transverse load is to be treated
L	panel length
M	bending moment, per unit width
M_x	applied bending moment per unit width (see figs. 2 and 7)
m	half-wavelength number, L/λ
MAXL	maximum number of values of λ for which buckling or frequency constraints are calculated
MINLAM	integer that specifies smallest value of λ for which buckling loads are examined ($\lambda = L/\text{MINLAM}$)
NEIG(m)	number of eigenvalues determined at $\lambda = L/m$

$N_x, N_y, N_{xy},$ NX, NY, NXY	inplane longitudinal, transverse, and shear loads per unit width, applied to panel
$N_{x_{cr}}$	value of N_x that corresponds to eigenvalue
$N_{x_{input}}$	input value of N_x ; also value of N_x for which panel is designed
N_{x_E}	Euler buckling load of panel
$N_{x_i}, N_{y_i},$ N_{xy_i}	inplane longitudinal, transverse, and shear loads per unit width, applied to plate element i
N_{xy_p}	shear load applied to substructure
$P, PRESS$	uniform lateral pressure
Q'_{jk}	lamina stiffnesses in material coordinate system, defined in equations (6) through (9)
Q'_{jT}, Q_{jT}	lamina properties associated with thermal expansion; primed quantities indicate material coordinate system; unprimed quantities indicate panel coordinate system
RHO	density
S	lamina stress or strain (see eq. (48))
S_{allow}	allowable value of S (see eq. (48))
S_i	shear flexibility for plate element i (see eq. (30))
S_p	shear flexibility for substructure p (see eqs. (31) and (33))
$SHEAR$	parameter used to indicate whether the standard VIPASA analysis is to be used for the $\lambda = L$ buckling load ($SHEAR = 0$) or whether the adjusted analysis is to be used ($SHEAR > 0$); appropriate only for cases where the loading involves shear
t	thickness

u, v, w	plate element displacements in local plate element coordinate system
X_i	sizing variable
\bar{X}_i	value of X_i at initial point of Taylor series expansion of constraints
x, y, z	coordinate directions in local plate element coordinate system; axes defined in figure 6
z_i	distance from reference surface to centroid of plate element i
z_i	distance from centroid of cross section to centroid of plate element i
$\alpha_1, \alpha_2,$ ALFA1, ALFA2	coefficient of thermal expansion of composite material in material coordinate system
γ	$F/F(\lambda = L)$
$\nabla T, \text{TEM}$	change in temperature
$\epsilon_x, \epsilon_y, \gamma_{xy}$	laminate strains in plate element coordinate system
θ, THET	angle between material coordinate system and plate element coordinate system (see figure 6)
$\nu_1, \nu_2, \text{ANUI}$	Poisson's ratios of composite material in material coordinate system
λ	buckling or vibration half-wavelength

DESCRIPTION OF GENERAL APPROACH USED IN AND CAPABILITY OF PASCO COMPUTER CODE

Overview

PASCO has been developed to aid the engineer in the analysis and sizing of prismatic structures such as those shown in figure 1. Because of their wide application in aerospace structures, stiffened panels are given special emphasis in PASCO. For example, complex panel configurations can be built up from a

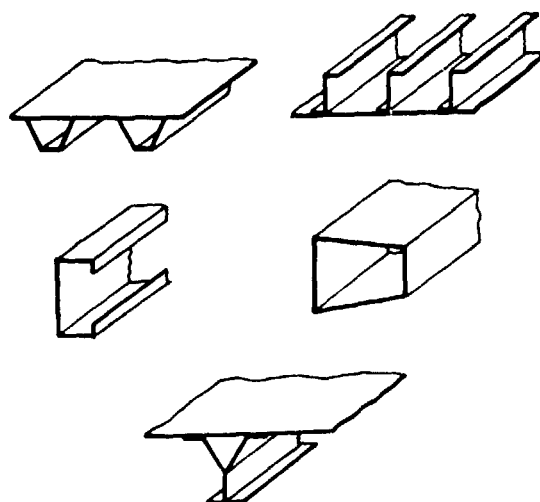


Figure 1.- Examples of typical structures.

a relatively small number of repeating elements, the loadings (figure 2) available in PASCO are the type usually associated with panels, and practical panel design considerations such as an overall bow-type initial imperfection (figure 3) can be accounted for.

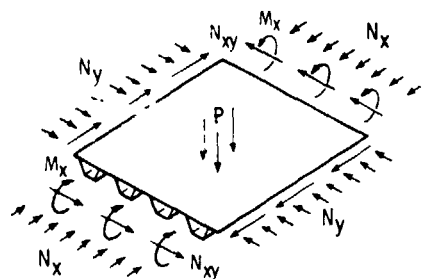


Figure 2.- Available loadings applied to hat-stiffened panel.

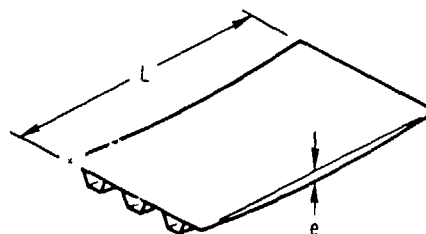


Figure 3.- Overall bow-type initial imperfection.

The panel cross section is composed of an arbitrary assemblage of thin, flat, rectangular plate elements that are connected together along their longitudinal edges. Each plate element consists of a balanced symmetric laminate of any number of layers of orthotropic material. Any group of element widths,

layer thicknesses, and layer orientation angles can be selected as sizing variables. For example, in the blade-stiffened panel configuration shown in figure 4, the blade depth can be allowed to vary, the overall stiffener spacing can be held fixed, the thickness of the material at the 0° and $\pm 45^\circ$ orientations can be allowed to vary, and the orientation angles themselves can be held fixed.

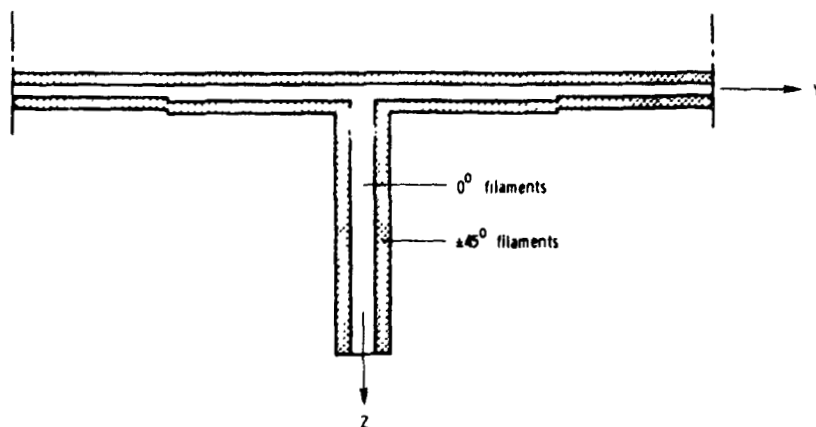


Figure 4.- Blade-stiffened panel configuration.

When used in the analysis mode, PASCO can be used to calculate laminate stiffnesses, lamina stresses and strains (including the effect of temperature), buckling loads, vibration frequencies, and overall panel stiffness. When used in the sizing mode, PASCO adjusts the sizing variables to provide a low-mass panel design that will carry a set of specified loadings without failure by buckling or material strength and that will meet other design requirements such as upper and lower bounds on sizing variables, upper and lower bounds on overall bending,

extensional and shear stiffness, and lower bounds on vibration frequencies.

Approach and Capability

The approach used in and the capability of PASCO are summarized in figure 5. The topics listed in figure 5 are discussed briefly here and are explained in greater detail in subsequent portions of the report.

DESIGN CONDITIONS

- N_x, N_y, N_{xy}, M_x
- Lateral pressure
- Bow-type imperfection
- Temperature
- Multiple sets of design conditions

ANALYSIS

- VIPASA for eigenvalues
- Prebuckling stresses include bending stresses caused by applied moment, lateral pressure, bow, temperature, and transverse load
- Lamina stresses and strains for strength criteria

PANEL CONFIGURATION AND MATERIAL

- General configuration
- Multiple materials
- Materials orthotropic at arbitrary angle
- Balanced, symmetric laminates
- Uniform along panel length
- Detailed modeling

SIZING, SIZING VARIABLES, AND CONSTRAINTS

- Nonlinear mathematical programming
- Minimize mass
- Sizing Variables: element widths, ply thickness, and ply orientation angle
- Sizing variable linking
- Bounds on sizing variables
- Constraints: buckling, material strength, stiffness, vibration frequency

Figure 5.- PASCO capability and approach.

Design conditions.- The design conditions considered are a loading of N_x , N_y , N_{xy} , and M_x , lateral pressure, an overall bow-type imperfection, and temperature. Lateral pressure and the bow are treated using a beam-column approach. Thermal stresses are calculated assuming that the temperature (or, more precisely, the change in temperature) is specified in each plate element. Temperature does not vary with the sizing variables. Panels can be sized for multiple sets of design conditions.

Analysis.- The eigenvalue analyses for buckling and vibration frequency are performed by a stiffened panel analysis code denoted VIPASA (refs. 6 and 7). The prebuckling stress state includes bending stresses caused by an applied bending moment, lateral pressure, an overall bow, temperature, and a transverse load. Resultant prebuckling lamina stresses and strains are calculated for the material strength criteria.

Panel configuration and material.- The panel cross section can have a general configuration. Each plate element can contain multiple orthotropic materials oriented at arbitrary angles. However, each plate element must be a balanced, symmetric laminate and must be uniform along its length. Many unsymmetric laminates can be generated by stacking plate elements composed of symmetric laminates. (This approach is discussed in reference 1.) Curved panels can be modeled using a series of flat plate elements. Provision for offsets and a large number of distinct layers in each laminate allow relatively detailed modeling of the panel cross section.

Sizing, sizing variables, and constraints.- Sizing is carried out using a nonlinear mathematical programming approach in which the design requirements are treated as inequality constraints. The objective function, the quantity that is minimized, is the panel mass per unit width. The panel length is fixed.

Any set of plate element widths, layer thicknesses, and layer orientation angles can serve as the sizing variables. The other plate element widths, layer thicknesses, and layer orientation angles can be held fixed or linked linearly to those that serve as sizing variables. During panel sizing, linking can be used to provide practical proportions, calculate offsets that change as thicknesses change, and maintain overall panel width.

The design requirements, or constraints, that can be specified are upper and lower bounds on sizing variables, lower bounds on buckling and material strength, upper and lower bounds on overall bending, extensional, and shear stiffnesses, and lower bounds on vibration frequency. Separate margins of safety can be placed on each buckling or vibration mode. Several material strength criteria are included, and, if desired, the user can incorporate his own material strength criterion by writing an additional subroutine.

STRUCTURAL ANALYSIS

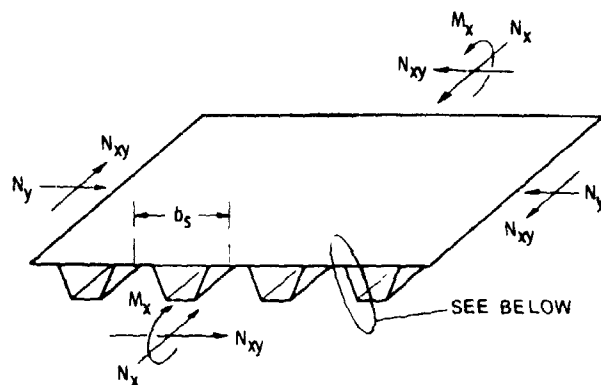
Analytical foundations for PASCO are discussed in terms of structural analysis and in terms of sizing. The focus of this section is structural analysis. Sizing is considered in a subsequent section.

Prebuckling Stress Analysis

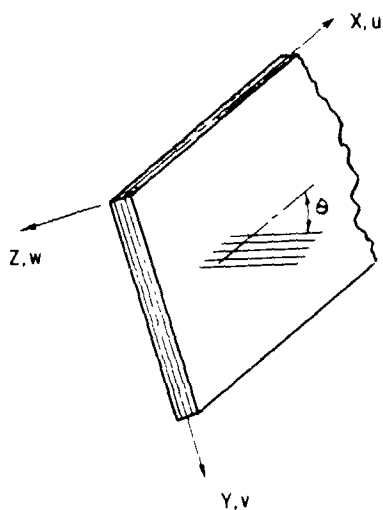
The prebuckling load distribution on each plate element is required for the buckling analysis and is used to compute lamina stresses and strains for the material strength criterion. The loads on each plate element are calculated using the following approach: The load distribution is first determined for a uniform longitudinal strain. Additional bending loads are then calculated and added to the load distribution determined for uniform longitudinal strain. Finally, the shear stress distribution is computed and added. Each of these steps is discussed in greater detail in subsequent sections of this report.

Elastic relations.- The elastic relations are presented for a plate element with coordinate system, displacements, and loading as shown in figure 6.

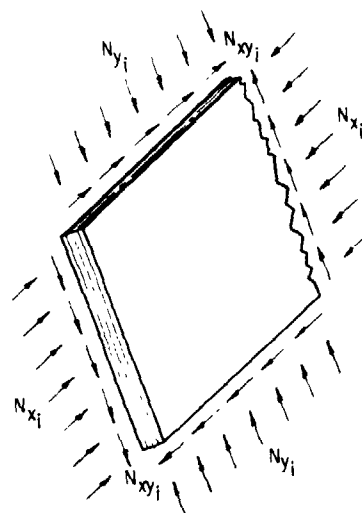
With the assumption of balanced, symmetric laminates, the general plate constitutive equations uncouple. The equations for inplane loads for plate element i reduce to



(a) Hat-stiffened panel with applied loading



(b) Plate element coordinate system, displacements, and ply orientation angle



(c) Plate element i with inplane loading. Directions shown are positive for prebuckling loads.

Figure 6.- Plate element coordinate system, displacements, loading, and sign convention.

$$\begin{bmatrix} N_{x_i} \\ N_{y_i} \\ N_{xy_i} \end{bmatrix} = \begin{bmatrix} A_{11} & A_{12} & 0 \\ A_{12} & A_{22} & 0 \\ 0 & 0 & A_{33} \end{bmatrix}_i \begin{bmatrix} \epsilon_x \\ \epsilon_y \\ \gamma_{xy} \end{bmatrix}_i + \begin{bmatrix} C_{1T} \\ C_{2T} \\ C_{3T} \end{bmatrix}_i \quad (1)$$

in which N_{x_i} , N_{y_i} , and N_{xy_i} are the inplane loads on plate element i (positive in compression); A_{jk} are laminate stiffnesses; ϵ_x , ϵ_y , γ_{xy} are strains (positive in compression) given by

$$\epsilon_x = - \frac{\partial u}{\partial x} \quad (2)$$

$$\epsilon_y = - \frac{\partial v}{\partial y} \quad (3)$$

$$\gamma_{xy} = - \left(\frac{\partial u}{\partial y} + \frac{\partial v}{\partial x} \right) \quad (4)$$

u and v are prebuckling displacements; and C_{jT} are the temperature terms given by

$$C_{jT} = \int Q_{jT} (\nabla T) dz \quad (5)$$

in which ∇T is the change in temperature. The change in

temperature ∇T is allowed to be ply dependent and, therefore, can vary with z .

For an orthotropic lamina with material coordinate system inclined at an angle θ to the plate element coordinate system (Fig. 6), the Q_{jT} are first calculated in the material coordinate system (the primed system) and then transformed to the plate element coordinate system as follows:

$$Q'_{11} = \frac{E_1}{1 - \nu_1 \nu_2} \quad (6)$$

$$Q'_{12} = \frac{\nu_2 E_1}{1 - \nu_1 \nu_2} = \frac{\nu_1 E_2}{1 - \nu_1 \nu_2} \quad (7)$$

$$Q'_{22} = \frac{E_2}{1 - \nu_1 \nu_2} \quad (8)$$

$$Q'_{33} = E_{12} \quad (9)$$

$$Q'_{1T} = Q'_{11} \alpha_1 + Q'_{12} \alpha_2 \quad (10)$$

$$Q'_{2T} = Q'_{12} \alpha_1 + Q'_{22} \alpha_2 \quad (11)$$

$$Q_{1T} = Q'_{1T} \cos^2 \theta + Q'_{2T} \sin^2 \theta \quad (12)$$

$$Q_{2T} = Q'_{1T} \sin^2 \theta + Q'_{2T} \cos^2 \theta \quad (13)$$

$$Q_{1T} = (Q'_{1T} - Q'_{2T}) \sin \theta \cos \theta \quad (14)$$

Uniform longitudinal strain.— With the assumption that the prebuckling longitudinal strain ϵ_x is uniform over the panel cross section, the strain ϵ_x is given by

$$\epsilon_x = \frac{N_x \cdot b_s - \sum C_i b_i}{\sum \bar{A}_i b_i} \quad (15)$$

in which N_x is the applied longitudinal load per unit width, b_s is the width of one period of the stiffened panel (fig. 6), the summation extends over all elements in a period, and

$$\bar{A}_i = A_{11} - (A_{12})^2/A_{22} \quad \text{for plate } i \quad (16)$$

$$b_i = \text{width of plate } i \quad (17)$$

$$C_i = A_{12}(N_y - C_{2T})/A_{22} + C_{1T} \quad \text{for plate } i \quad (18)$$

The longitudinal loading N_{x_i} in plate i is then given by

$$N_{x_i} = \epsilon_x \bar{A}_i + C_i \quad (19)$$

In the expression for C_i , the transverse load N_{y_i} in plate i can be determined two ways. One way is to use the PASCO modeling rules discussed in reference 1. The other way is to specify the values of N_{y_i} with program input. In general, the modeling rules are designed so that the full N_y is carried by the skin, and no N_y is carried by the stiffener elements.

Note that even though the longitudinal strain ϵ_x is uniform, the term C_i in equation (19) may produce a net bending moment about the centroid of the panel cross section.

Bending loads.- In this section, expressions for bending strains caused by various loadings are developed. These bending strains are combined with the uniform strains from equation (15) to calculate the total axial loading N_{x_i} in each plate element. Bending loads can be caused by an applied bending moment, a bow-type imperfection, lateral pressure, temperature, and/or an applied transverse load. These bending loads are calculated by PASCO and, except for those bending loads already included in C_i (eq. (18)), are added to the longitudinal load distribution given by equation (19). Certain options involving the bending loads produced by temperature and/or an applied transverse load are discussed later in this section.

For combinations of applied moment, lateral pressure, and initial bow, the maximum bending moment, which occurs at panel midlength, is given as in reference 8 by

$$M = M_x + \frac{N_x \cdot e}{1 - \gamma} + \frac{PL^2}{\pi^2} \frac{1}{\gamma} \left[\sec\left(\frac{\pi}{2}\sqrt{\gamma}\right) - 1 \right] \quad (20)$$

where

$$\gamma = \frac{N_x}{N_{x_E}} \quad (21)$$

and N_x is the applied longitudinal load, N_{x_E} is the Euler buckling load for the panel, M_x is the applied bending moment on the panel, e is the bow at panel midlength, P is the lateral pressure loading, and L is the panel length. Most of these quantities, together with the overall panel coordinate system, are shown in figure 7. Note that the bending load caused by the applied bending moment M_x is not influenced by inplane loads.

Because the VIPASA buckling analysis requires that the stress distribution be constant along the panel length, the conservative assumption is made that the bending moment given by equation (20) is the bending moment over the entire panel length.

For buckling modes having a half-wavelength λ equal to the panel length L , the bending moments caused by a bow and/or lateral pressure are omitted from equation (20). Only the applied bending moment M_x is retained.

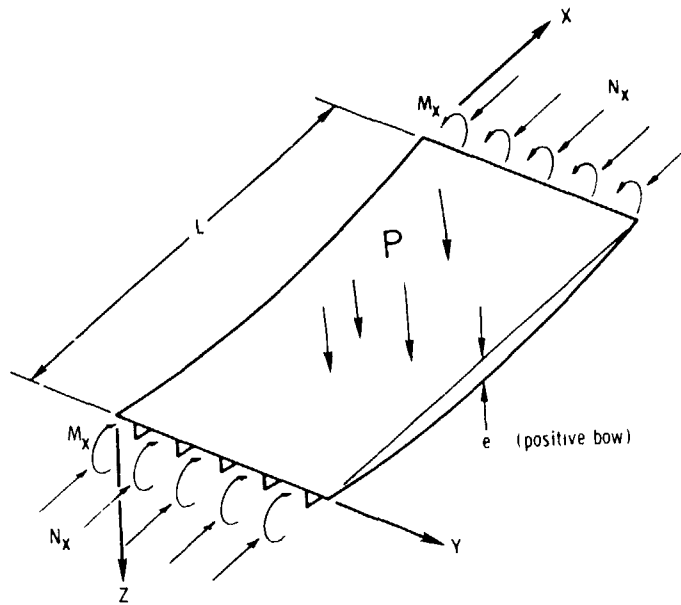


Figure 7.- Panel with applied bending moment, initial bow, and lateral pressure.

Strictly speaking, equations (20) and (21) are appropriate only when N_x is the sole inplane loading; however, in PASCO, these equations are applied to problems with combined loads. For combined loads, the parameter γ is defined as

$$\gamma = \frac{F}{F(\lambda \approx L)} \quad (22)$$

in which F is a scalar defined by

$$F \begin{bmatrix} N_x \\ N_y \\ N_{xy} \\ P \\ M_x \\ \nabla T \\ f \end{bmatrix}_{\text{input}} = \begin{bmatrix} N_x \\ N_y \\ N_{xy} \\ P \\ M_x \\ \nabla T \\ f \end{bmatrix}_{\text{buckling or vibration}} \quad (23)$$

The input vector on the left, which is the design loading and frequency requirement, is scaled up or down with the parameter F to obtain that combination that causes buckling or vibration.¹ Since there is a question about the validity of equation (20) in the case of combined loads, and since it would be inappropriate to use a frequency requirement to calculate γ for equation (20), a user should exercise caution in the application of equation (20) to calculate bending loads. For the latter reason, subsequent discussions in this section will focus on buckling.

During the buckling analysis, the buckling load is calculated for many values of buckling half-wavelength λ , and more than one buckling load can be calculated at a given value of λ . There is a value of F associated with each of these buckling loads. In equation (22), $F(\lambda = L)$ is the value of F associated with the lowest buckling load for $\lambda = L$. The value used for F in the numerator of equation (22) depends upon whether the bending moment in equation (20) is to be used for material strength calculations or buckling calculations.

- For material strength calculations, the bending moment that is used to calculate lamina stresses and strains is based on one of two values of F for the numerator of equation (22).

¹A more complete discussion of F is presented in a subsequent section entitled FACTOR and F .

(1) If $F(\lambda = L)$ is greater than 1.0, then $F = 1.0$.

(2) If $F(\lambda = L)$ is equal to or less than 1.0, then F is the value of F for the minimum buckling load for λ considered.

- For buckling calculations, F that appears in the numerator of equation (22) is the value of F associated with the eigenvalue number and buckling half wavelength being examined. The resulting bending moment is used to calculate prebuckling plate element loads.

In the discussion following equation (19), it was pointed out that the C_i term, which accounts for temperature and transverse loads, can produce a bending moment in the panel. This bending moment is treated in PASCO in one of two ways:

(1) the panel is allowed to take on a bow (JTHERM=1), or (2) the panel is forced to remain flat (ITHERM=0). If the panel is allowed to take on a bow, the magnitude of the bow is calculated to produce zero bending moment in a panel loaded only by temperature and transverse loads. This bow is then added to any initial bow that exists in the panel. If the panel is forced to remain flat, no additional bow is added and any bending moment produced by the C_i terms in equation (19) is retained. The user selects the desired approach with the input parameter ITHERM.

The treatment of the bending moment caused by C_i can also be described in the following way. Let a moment M be defined by

$$M = M_x + \frac{N_x(e + e_c)}{1 - \gamma} + \frac{PL^2}{\gamma\pi^2} \left[\sec\left(\frac{\pi}{2}\sqrt{\gamma}\right) - 1 \right] - M_c \quad (24)$$

in which e_c and M_c are the only terms that do not appear in equation (20). The quantity e_c is the magnitude of a bow calculated to produce zero bending moment in a panel loaded only by temperature and transverse loads, and M_c is the moment caused by C_i (eq. (18)). When ITERM is set equal to 1 with program input, the bending moment that is added to the stress state associated with uniform strain is given by equation (24). When ITERM is set equal to 0 with program input, the bending moment that is added to the stress state associated with uniform strain is given by equation (20).

Bending loads are applied to the panel with an N_{x_i} loading that varies by steps in the z direction. An example is shown in figure 8. In this example, a blade-stiffened panel is subjected to longitudinal compression and a bending moment that puts the skin in additional compression. The blade is modeled as three separate plate elements. The moment-induced N_{x_i} load in each plate element, including the skin, is calculated by assuming that (1) the strain at the centroid of each plate element forms a "linear" strain distribution, (2) the net inplane load caused by the bending strain is zero, and (3) the net bending moment produced by bending strains is equal to the calculated moment. The resulting bending strain distribution is given by

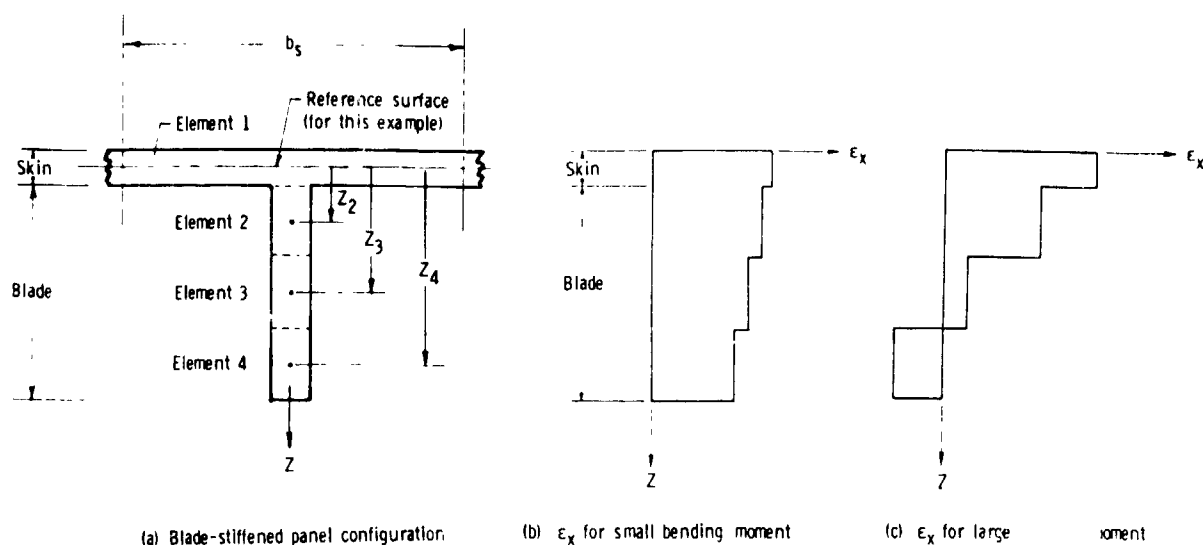


Figure 8.- Idealized longitudinal strain distributions on compression panels with bending moment.

$$\epsilon_{M_i} = (\epsilon_A + \epsilon_B z_i) M \quad (25)$$

in which ϵ_{M_i} is the bending strain in element i , z_i is the distance from the reference surface to the centroid of plate element i (fig. 8), and

$$\epsilon_A = -\epsilon_B \frac{\sum \bar{A}_i b_i z_i}{\sum \bar{A}_i b_i} \quad (26)$$

$$\epsilon_B = \frac{b_s}{\sum \bar{A}_i b_i (z_i)^2 - \frac{[\sum \bar{A}_i b_i z_i]^2}{\sum \bar{A}_i b_i}} \quad (27)$$

$$\bar{A}_i = A_{11} - (A_{12})^2/A_{22} \quad \text{for plate element } i \quad (28)$$

The summations are over all elements in one period of the stiffened panel, and b_s is the width of one period.

The bending strains ϵ_{M_i} from equation (25) are combined with the uniform longitudinal strain ϵ_x from equation (15) to produce the resultant longitudinal loading in each element

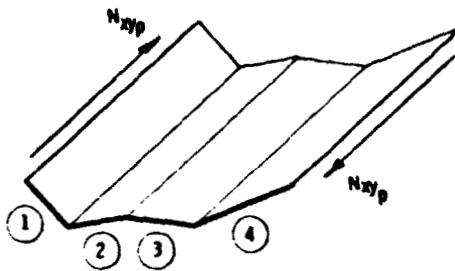
$$N_{x_i} = (\epsilon_{M_i} + \epsilon_x) \bar{A}_i + C_i \quad (29)$$

Shear stress.— The shear stress in each plate element is calculated using a generalization of the approach of reference 5 in which equilibrium and compatibility of displacement are employed. Define a shear flexibility S_i for a plate of width b_i

$$S_i = b_i/A_{33_i} \quad (30)$$

For plates or substructures connected in series, (Fig. 9), the shear flexibility S_p for the substructure is given by

$$S_p = S_1 + S_2 + \dots + S_n \quad (31)$$



① Plate element or substructure number

Figure 9.- Plate elements or substructures connected in series.
and the shear in each plate or substructure is

$$N_{xy1} = N_{xy2} = \dots = N_{xyn} = N_{xyp} \quad (32)$$

in which N_{xyp} is the shear load on the substructure.

For plates or substructures connected in parallel (fig. 10),
the shear flexibility S_p is given by

$$1/S_p = 1/S_1 + 1/S_2 + \dots + 1/S_n \quad (33)$$

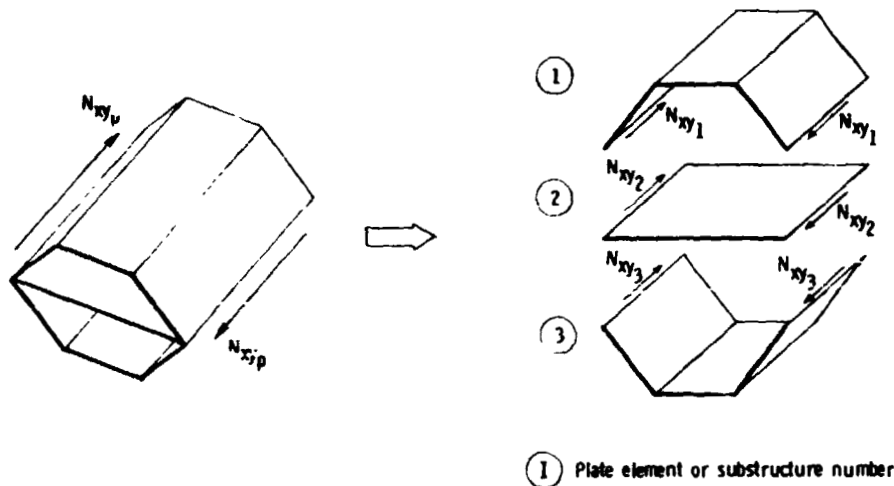


Figure 10.- Plate elements or substructures connected in parallel.

and

$$\frac{N_{xy_i}}{N_{xy_p}} = \frac{S_p}{S_i} \quad (34)$$

In PASCO, the overall panel shear stiffness is calculated by VIPASA. However, the N_{xy_i} and S_i given above could be used to calculate a total shear angle which, in turn, could be used to define an overall panel shear stiffness. Usually, the two approaches give results in close agreement.

The shear stress in any element can also be specified by the user with program input.

VIPASA Buckling Analysis

Buckling and vibration analyses in PASCO are carried out with a stiffened panel analysis code denoted VIPASA (Vibration and Instability of Plate Assemblies including Shear and Anisotropy) described in references 6 and 7. For simplicity, only buckling terminology is used in the present discussion of VIPASA. It is understood, however, that the discussion also applies to the vibration analysis.

The VIPASA analysis treats an arbitrary assemblage of plate elements with each plate element i loaded by N_{x_i} , N_{y_i} , and N_{xy_i} . The buckling analysis connects these individual plate elements and maintains continuity of the buckle pattern across the intersection of neighboring plate elements. Several

buckling modes are shown in figures 11 and 12. VIPASA considers only initial buckling. Postbuckling response is not considered by VIPASA or PASCO.

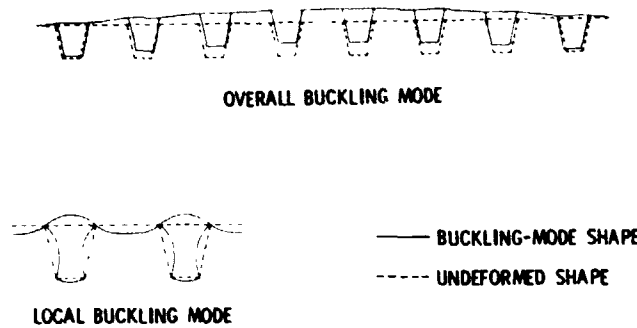


Figure 11.- Typical buckling modes for hat-stiffened panel.

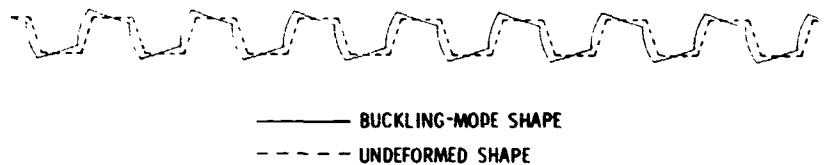


Figure 12.- Typical buckling mode for corrugated panel.

Elastic relations.- In the VIPASA analysis, a local coordinate system is defined for each individual plate element. In the example shown in figure 6, the X, Y, Z axes define the local coordinate system in the local longitudinal, transverse, and lateral directions, respectively. The buckling displacements u, v, and w are defined in this local coordinate system and are the same as those shown in figure 6.

During buckling, the out-of-plane elastic deformations of each plate element are defined by

$$\begin{bmatrix} M_{x_i} \\ M_{y_i} \\ M_{xy_i} \end{bmatrix} = - \begin{bmatrix} D_{11} & D_{12} & D_{13} \\ D_{12} & D_{22} & D_{23} \\ D_{13} & D_{23} & D_{33} \end{bmatrix}_i \begin{bmatrix} \frac{\partial^2 w}{\partial x^2} \\ \frac{\partial^2 w}{\partial y^2} \\ 2 \frac{\partial^2 w}{\partial x \partial y} \end{bmatrix}_i$$

(35)

where M_{x_i} , M_{y_i} , and M_{xy_i} are perturbation bending and twisting moments per unit length on plate element i , D_{jk} are the laminate stiffnesses, and w is the perturbation displacement in the z -direction. Because of the requirement that each plate element consist of a balanced, symmetric laminate,² anisotropic effects are limited to those produced by the D_{13} and D_{23} terms. Therefore, in subsequent discussions, anisotropy refers only to anisotropy in the bending stiffness.

²VIPASA does not require that plate element laminates be balanced and symmetric. However, as can be seen from equations (1) and (35), VIPASA ignores extension-shear coupling and membrane-bending coupling in each plate element. The resulting elastic relations are the same as those that are obtained for a laminate that is balanced and symmetric. Because of the elastic relations in VIPASA and because balanced and symmetric laminates are the most common laminates in aerospace applications, PASCO input provides only balanced, symmetric laminates for each plate element. By stacking symmetric laminates (ref. 1), many unsymmetric laminates can be modeled and the coupling action in the elastic response for these unsymmetric laminates can be accounted for.

Buckling displacements and boundary conditions.- The buckling displacement w assumed in VIPASA for each plate element is

$$w = \text{Re} \left[F(y) e^{i\pi x/\lambda} \right] \quad (36)$$

with similar expressions assumed for the inplane displacements u and v . For $F(y)$ written as

$$F(y) = f_1(y) + if_2(y) \quad (37)$$

the buckling displacement w can be written as

$$w = f_1(y) \cos \frac{\pi x}{\lambda} - f_2(y) \sin \frac{\pi x}{\lambda} \quad (38)$$

Neglecting boundary conditions, the displacement shape assumed in equation (38) provides an exact solution to the governing differential equations if the panel and loading are uniform in the x -direction. The governing equations are based on the Kirchhoff-Love hypothesis applied to each plate element.

The functions $f_1(y)$ and $f_2(y)$ allow various boundary conditions to be prescribed on the lateral edges of the panel. These boundary conditions, which include free, simple support, clamped, and symmetry, are discussed in the users manual, reference 1. Boundary conditions cannot, however, be prescribed on the ends of the panel.

Orthotropic panels with no shear loading.- For orthotropic panels with no shear loading, f_2 , the imaginary part of $F(y)$, is zero. The solution $f_1(y) \cos \frac{\pi x}{\lambda}$ provides a series of node lines that are straight, perpendicular to the longitudinal panel axis, and spaced λ apart as shown in figure 13. Along each of these node lines, the buckling displacements satisfy the following simple support boundary conditions: u is unrestrained, $v = w = 0$, and $w_{,x}$ is unrestrained. For values of λ given by $\lambda = L, L/2, L/3, \dots L/m$, where L is the panel length and m is an integer, the nodal pattern shown in figure 13 provides simple support boundary conditions at the ends of a finite, rectangular panel. An example in which $\lambda = L/2$ is shown in figure 14.

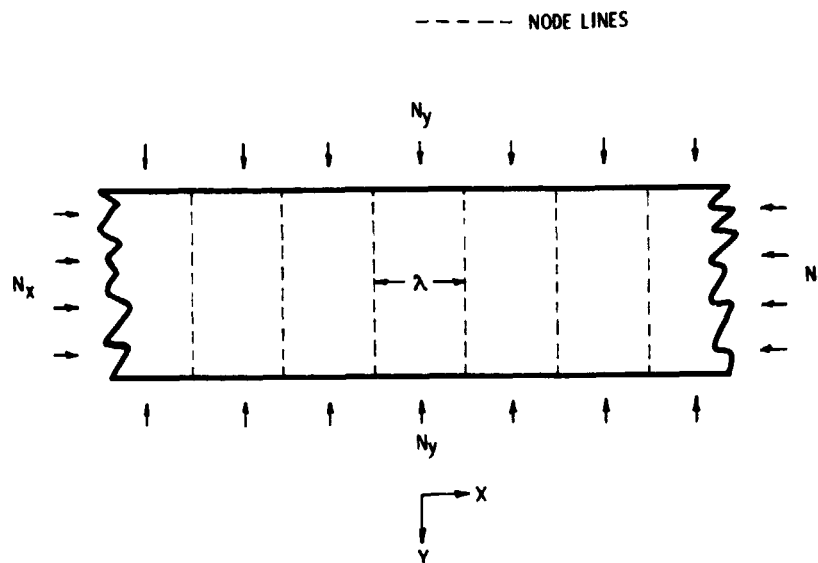


Figure 13.- Node lines produced by $w = f_1(y) \cos \frac{\pi x}{\lambda}$ for orthotropic panels with no shear loading.

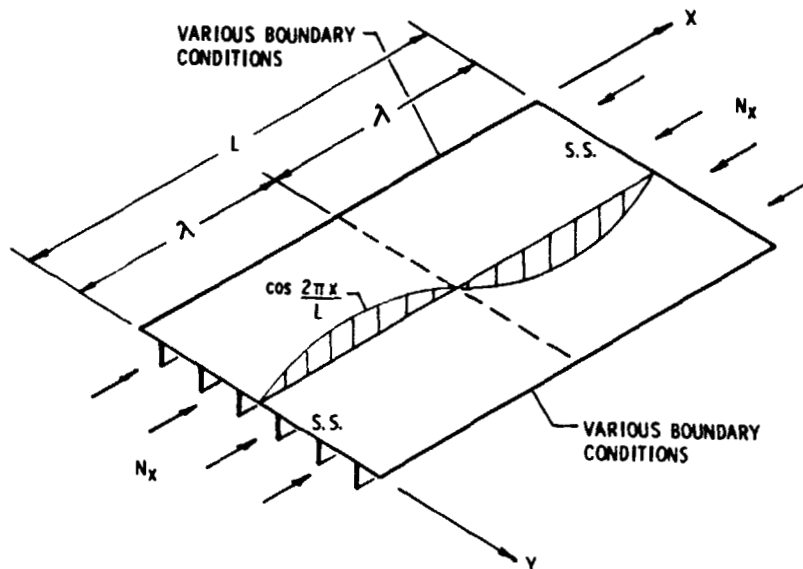


Figure 14.- Buckling of orthotropic panel under longitudinal loading. Mode shown is $m = 2$.

Anisotropic panels and/or panels with a shear loading.- For anisotropic panels and/or panels with a shear loading, $f_2 \neq 0$. The functions f_1 and f_2 are such that node lines are skewed and not straight, but the node lines are still spaced λ apart as shown in figure 15. In this case, the solution given by equation (38) is accurate only when many buckles form along the panel length, in which case boundary conditions at the ends are not important. An example in which $\lambda = L/4$ is shown in figure 16.

As λ approaches L , the VIPASA buckling analysis for a panel loaded by N_{xy} can be quite conservative. One explanation is as follows: As can be seen in figure 16, the skewed nodal lines given by VIPASA in the case of shear and/or anisotropy do not coincide with the end edges. Forcing node lines to

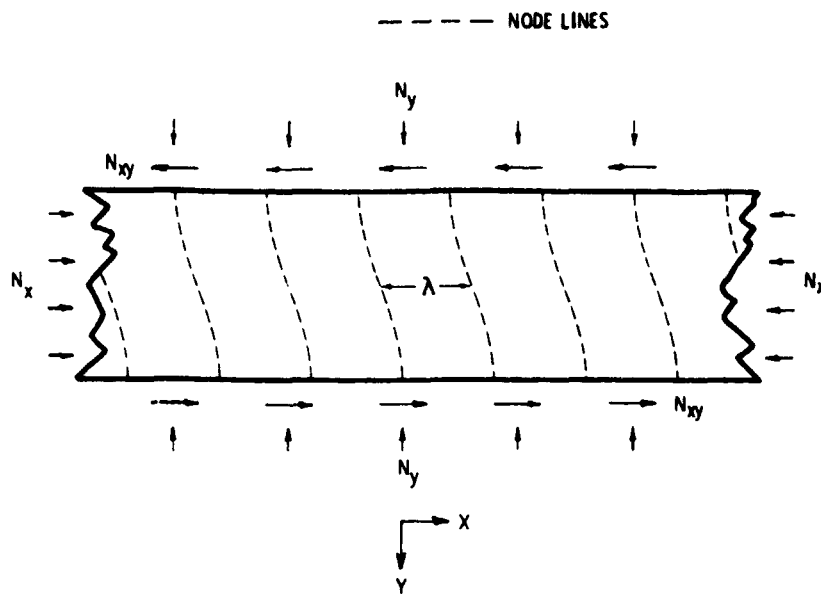


Figure 15.- Node lines produced by $w = f_1(y) \cos \frac{\pi X}{\lambda} - f_2(y) \sin \frac{\pi X}{\lambda}$ for anisotropic panels and/or panels with a loading that includes shear.

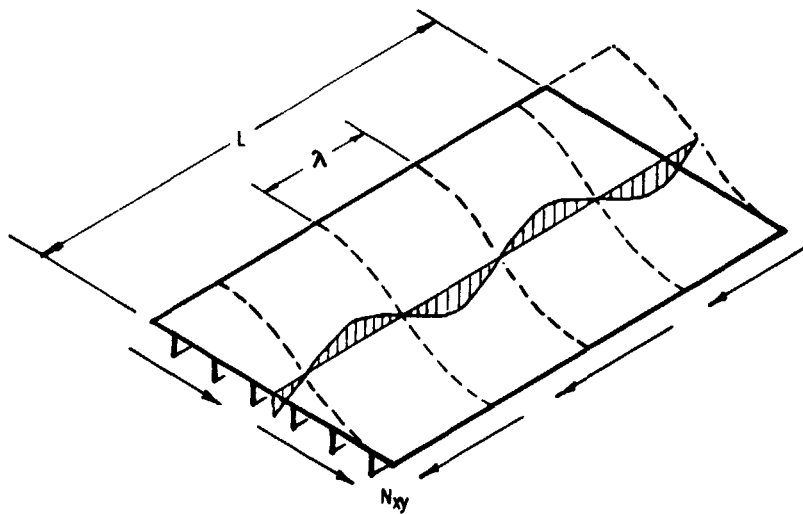


Figure 16.- Buckling of panel under shear loading.
Mode shown in $m = 4$.

coincide with the end edges produces long-wavelength buckling loads that are, in many cases, appreciably higher than those determined by VIPASA. Calculations have shown that for long-wavelength buckling modes, the effect of anisotropy is minimal for most practical cases. Anisotropy therefore, causes negligible conservatism in a VIPASA analysis. The presence of a shear loading can, however, lead to very conservative results for λ equal to L . (See, for example, ref. 9.)

Because of VIPASA's conservatism in the case of long-wavelength buckling if a shear load is present, an adjusted shear analysis procedure can be used (at the user's option) for the case $\lambda = L$. That adjusted analysis is discussed in a subsequent section entitled Adjusted Analysis for Shear Buckling.

Example.- A buckling response diagram, such as that shown in figure 17, provides a convenient means of studying the buckling response of a panel and can be used to help explain some of the features of the buckling analysis and the computer code. The example shown in figure 17 is for a blade-stiffened panel having arbitrary but reasonable proportions. The panel has a length L of 0.76m (30 in.) and is modeled with 16 stiffeners. The boundary conditions on the lateral edges of the panel are taken to be simple support. Anisotropy is ignored. The loading on the panel is pure longitudinal compression; transverse and shear loads are taken to be zero. In the diagram, the buckling load N_{xcr} is given as a function of the

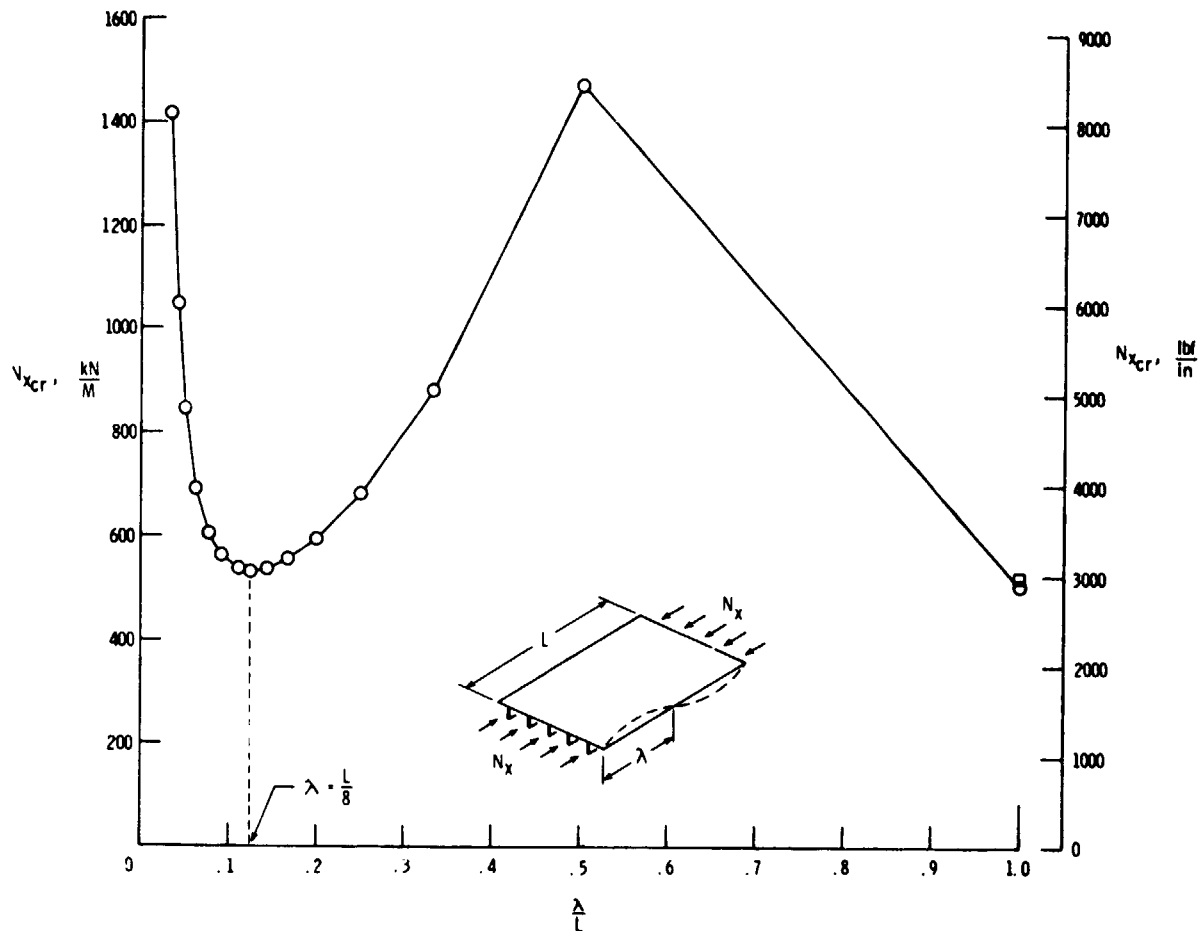
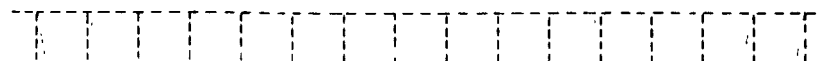
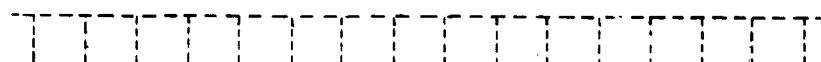


Figure 17.- Longitudinal buckling load as a function of buckling half-wavelength for blade-stiffened panel.

nondimensional half-wavelength λ/L . The half-wavelengths examined by PASCO are $\lambda = L, L/2, L/3, L/4, \dots, L/\text{MINLAM}$ in which MINLAM is program input. For this example, the lowest buckling load has a half-wavelength $\lambda = L$. The buckling mode shape for this mode is shown in figure 18a. The next lowest buckling load is a relative minimum that occurs for $\lambda = L/8$. The mode shape for this local mode is shown in figure 18b.



(a) OVERALL MODE, ($\lambda=L$)



(b) LOCAL MODE, ($\lambda=L/8$)

—— BUCKLING MODE SHAPE
 ---- UNDEFORMED SHAPE

Figure 18.- Buckling mode shapes for blade-stiffened panel example.

Although the program makes simple, exploratory calculations for many values of λ ($\lambda = L, L/2, L/3, \dots, L/\text{MINLAM}$), it calculates the buckling load for only certain values of λ . The program always calculates the buckling load for $\lambda = L$. The program also calculates the buckling load for specified values of λ given by $\lambda = L/\text{NLAM}$ where the vector parameter NLAM is input. (In order to obtain the data for figure 17, the vector NLAM was set equal to NLAM = 2, 3, 4, 5, \dots , 30.) In addition, the program calculates any buckling load which is a relative minimum ($\lambda = L/8$ in figure 17) that is lower than the next preceding calculated buckling load. Wavelengths are considered in order of decreasing length: $L, L/2, L/3, \dots, L/\text{MINLAM}$. Referring again to the example of figure 17, if no value of NLAM were input, the only buckling load calculated would be for

$\lambda = L$. The buckling load at the relative minimum $\lambda = L/8$ would not be calculated because that buckling load is greater than the next preceding calculated buckling load, which is at $\lambda = L$. If, on the other hand, NLAM = 2 were input, then the buckling loads would be calculated for $\lambda = L$, $\lambda = L/2$, and $\lambda = L/8$. The buckling load would be calculated for $\lambda = L/8$ because it is a relative minimum and because it is lower than the next preceding calculated buckling load - the load for $\lambda = L/2$.

The program input parameter NEIG(m) can be used to calculate more than one buckling eigenvalue at a given value of λ . Element m in vector NEIG(m) is the number of eigenvalues requested at a half-wavelength of $\lambda = L/m$. For example, for two eigenvalues at $\lambda = L$, the input is NEIG(1) = 2. In figure 17, the second eigenvalue at $\lambda = L$ is indicated by the square symbol at $\lambda = L$.

As explained earlier, PASCO can also account for an overall bow-type initial imperfection. The buckling response curves shown in figure 19 are for the same blade-stiffened panel discussed above, but with three different assumptions regarding an overall bow: (1) a positive bow of $e/L = +0.003$, (2) a negative bow of $e/L = -0.003$, and (3) a zero bow, $e/L = 0.0$. As in figure 17, the only loading is longitudinal compression. The curve for $e/L = 0.0$ is the same as that shown in figure 17. The bow does not directly affect the buckling load for $\lambda = L$. For this reason, the panel has the same buckling load at $\lambda = L$ for the

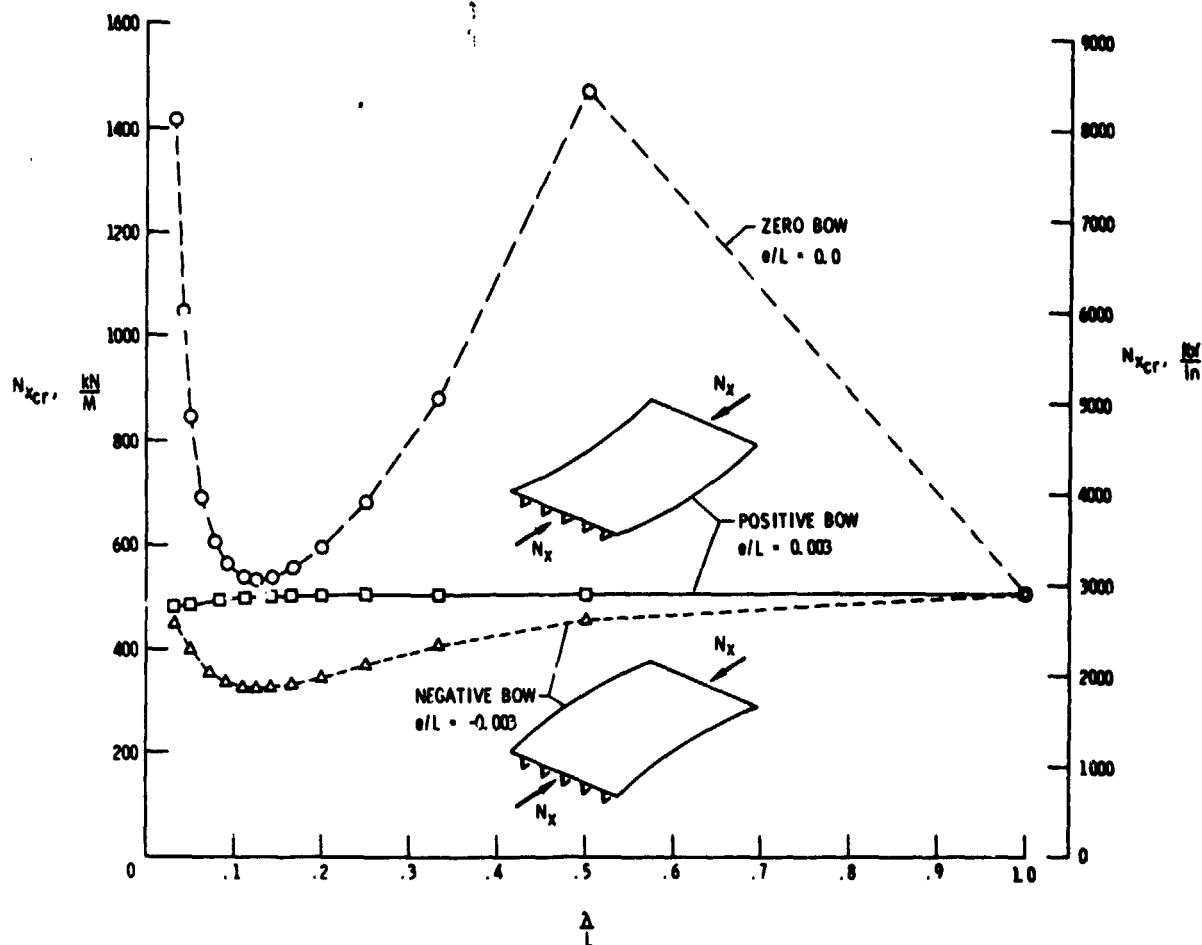


Figure 19.- Longitudinal buckling load as a function of buckling half-wavelength for blade-stiffened panel with positive bow, negative bow, and zero bow.

positive, negative, or zero bow. For a positive bow, which causes additional compression in the skin, the lowest buckling load occurs at $\lambda = L/30$. For a negative bow, which causes additional compression in the tip of the blade, the lowest buckling load occurs for $\lambda = L/8$.

FACTOR and F

In VIPASA, FACTOR is the unknown in the eigenvalue analysis. The desired eigenvalue is identified by half-wavelength λ and

by the eigenvalue number at that value of λ . A buckling analysis in VIPASA is merely an eigenvalue analysis at zero frequency.

The eigenvalue solution technique in VIPASA can be summarized as follows. For any set of values of FACTOR and half-wavelength λ , mathematical expressions in VIPASA provide the number of eigenvalues exceeded. Using this information, an iterative scheme in VIPASA identifies two values of FACTOR that bracket the desired eigenvalue. The difference between these two values of FACTOR can be made arbitrarily small, depending upon PASCO convergence criteria input CONV1 and CONV2.

In this report, a quantity is introduced that has essentially the same meaning as FACTOR. That quantity is denoted F. The quantities FACTOR and F differ in that whereas FACTOR is always the solution of an eigenvalue analysis in VIPASA and is identified with the word FACTOR in the VIPASA printout, F may not be the solution of a VIPASA eigenvalue analysis if an adjusted shear analysis is used in PASCO. Otherwise, FACTOR and F are identical.

For all analyses in PASCO, the scalar F is defined by

$$F \begin{bmatrix} N_x \\ N_y \\ N_{xy} \\ P \\ M_x \\ \nabla T \\ f \end{bmatrix}_{\text{input}} = \begin{bmatrix} N_x \\ N_y \\ N_{xy} \\ P \\ M_x \\ \nabla T \\ f \end{bmatrix}_{\text{eigenvalue}} \quad (39)$$

in which N_x , N_y , and N_{xy} are inplane loads, P is the lateral pressure, M_x is a bending moment, VT is a change in temperature, and f is a frequency. Whereas VIPASA can have a fixed load system that is added to the left side of equation (39), PASCO does not allow fixed loads. The entire input vector N_x to \bar{L} in equation (39) is scaled up or down with the quantity F to obtain the vector that provides the desired eigenvalue. The change in temperature represented by VT in equation (39) is ply dependent and can, therefore, be made to vary throughout the structure. In equation (39), the product of F and VT indicates the scaling of that distribution.

During the eigenvalue analysis, eigenvalues can be calculated for many values of half-wavelengths λ , and more than one eigenvalue can be calculated at a given value of λ . There is a value of F associated with each of these eigenvalues.

As an example, assume that the only two nonzero elements in the input vector on the left side of equation (39) are N_x and f . The response of a stiffened panel might be similar to that shown in figure 20. The solid curve indicates combinations of N_x and f that give the lowest eigenvalue. The value of N_x that causes buckling is $N_{x_{cr}}$; the natural frequency of the unloaded panel is f_n . Let the input values of N_x and f be represented by the solid circular symbol. The dashed line that passes through both the origin and the circular symbol indicates the locus of values of N_x and f that are considered by VIPASA as possible solutions to the eigenvalue problem. The

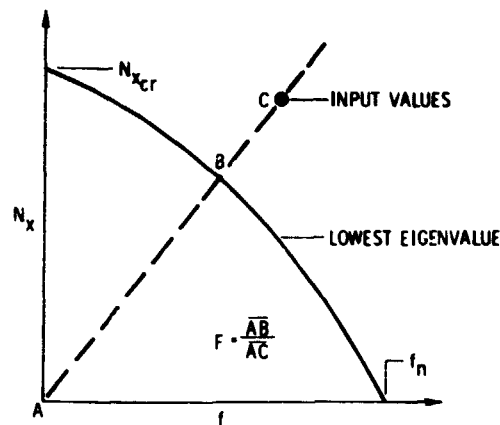


Figure 20.- Response of hypothetical stiffened panel showing combinations of N_x and f that provide the lowest eigenvalue, and a geometric interpretation of F .

direction cosines of this line are defined by the input values represented by the circular symbol. The unknown is the distance from the origin to the point at which the dashed line intersects the solid curve. This unknown is denoted F and can be thought of as the ratio of the distance \overline{AB} from the origin to the solid curve to the distance \overline{AC} from the origin to the circular symbol. In this hypothetical example, F is approximately 0.75. Other examples, involving combined loads with or without vibration frequency, are treated in the same manner.

Smeared Orthotropic Stiffnesses

Six smeared orthotropic stiffnesses are calculated by PASCO and are included in the output. These stiffnesses are denoted

- A_{11} longitudinal extensional stiffness
- A_{22} transverse extensional stiffness
- A_{33} shear stiffness
- D_{11} longitudinal bending stiffness

- D_{22} transverse bending stiffness
- D_{33} effective twisting stiffness

The stiffnesses A_{22} , A_{33} , and D_{22} are calculated within VIPASA using the VIPASA stiffness matrix, which relates forces and moments along the edges of a repeating element to the corresponding displacements and rotations. The stiffness matrix is evaluated at $F = 0$, $\lambda = \text{FSTIFF} \cdot L$ (where FSTIFF is input, default = 10) to approach the result obtained for a uniform edge loading. These stiffnesses are equivalent to the corresponding stiffnesses in the laminate force - distortion relationships given in equations (1) and (35).

The stiffnesses A_{11} , D_{11} , and D_{33} are not calculated within VIPASA, but are, instead, calculated with formulas as follows:

The smeared extensional stiffness A_{11} is defined as an ET-type stiffness given by

$$A_{11} = \frac{1}{b_s} \sum_i \left[A_{11i} - \frac{(A_{12i})^2}{A_{22i}} \right] b_i \quad (40)$$

in which the subscript i refers to plate element i , the A_{jk} are laminate stiffnesses defined by equation (1), the summation extends over all elements in one period of the stiffened panel, and b_s is the width of one period.

The smeared orthotropic bending stiffnesses D_{11} , D_{22} , and D_{33} are appropriate to use in the following differential

equation for lateral deflection of an orthotropic plate with lateral loading q .

$$D_{11} \frac{\partial^4 w}{\partial x^4} + 4D_{33} \frac{\partial^4 w}{\partial x^2 \partial y^2} + D_{22} \frac{\partial^4 w}{\partial y^4} = q \quad (41)$$

The smeared bending stiffness D_{11} is an EI-type stiffness given by

$$D_{11} = \frac{1}{b_s} \sum_i \left(A_{11i} - \frac{(A_{12i})^2}{A_{22i}} \right) \left(b_i z_i^2 + \frac{b_i^3}{12} \sin^2 \theta \right) + b_i D_{11i} \cos^2 \theta \quad (42)$$

in which z_i is the distance from the centroid of the cross section to the centroid of plate element i , and θ is the angle plate element i makes with the horizontal.

The formula for calculating the effective twisting stiffness D_{33} depends upon whether the panel is an open-section panel, such as a blade-stiffened panel, or a closed-section panel, such as a hat-stiffened panel. For open-section panels D_{33} is given by

$$D_{33} = \frac{1}{b_s} \sum_i b_i \left(\frac{1}{2} D_{12_i} + D_{33_i} \right) \quad (43)$$

in which the summation extends over all elements in one period of the stiffened panel, and the D_{jk} are laminate stiffnesses defined in equation (35). The D_{12} term is included in equation (43) to make D_{33} correct for equation (41). For closed-section panels, D_{33} is given by

$$D_{33} = \frac{\bar{A}^2}{b_s \sum_i \frac{b_i}{A_{33_i}}} \quad (44)$$

in which \bar{A} is the area enclosed by the closed section in one period and the summation extends only over those elements making up the closed section.

Adjusted Analysis for Shear Buckling

Rationale for adjusted analysis approach.- With the VIPASA analysis, the boundary conditions on the side edges (the edges parallel to the stiffeners in figure 21) can be specified and modeled correctly. However, the boundary conditions on the end edges (the edges normal to the stiffeners in figure 21) cannot be specified. The boundary conditions on the ends arise from the displacement shape assumed in equation (38). In the case of

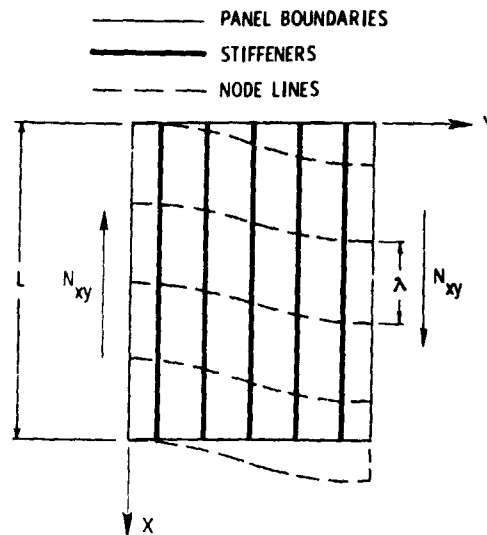


Figure 21.- Node lines determined by VIPASA in the case of a shear loading.

of loadings involving shear, the displacement shape and resultant nodal pattern produce boundary conditions on the ends that are not compatible with a finite rectangular panel. This incompatibility causes VIPASA to underestimate the $\lambda = L$ buckling load when the loading involves shear.

The adjusted shear analysis is an attempt to "rectangularize" the nodal pattern for the $\lambda = L$ buckling load and, thereby, provide a more accurate $\lambda = L$ buckling analysis for loadings involving shear. It is assumed that node lines would be more compatible with a finite rectangular panel if boundary conditions were modeled correctly on edges normal to the stiffeners than if boundary conditions were modeled correctly on edges parallel to the stiffeners. This assumption follows from the belief that, in such an analysis, the stiffeners would tend to produce node lines that are generally parallel to the stiffeners, as shown in

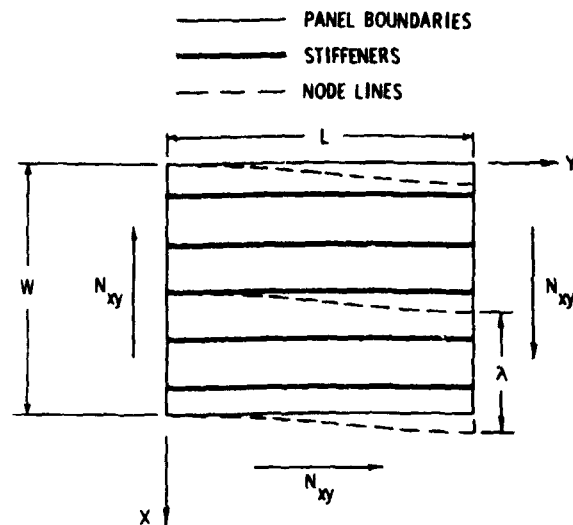


Figure 22.- Node lines for hypothetical VIPASA shear buckling solution for stiffened panel rotated 90°.

figure 22. It might appear that such an analysis could be carried out with VIPASA if the stiffened panel were first simply rotated 90°. However, VIPASA cannot solve this analysis problem because the VIPASA solution (eq. (38)) requires that the trigonometric solution be in the direction in which the panel is uniform, which, for a stiffened panel, is in the stiffener direction. Let the value of F for this target problem be denoted $F_{d,90}$, where F is defined in equation (39), d refers to discrete stiffeners, and 90 refers to the panel rotated by 90°.

Calculation of adjusted buckling load.- Although VIPASA cannot calculate $F_{d,90}$, VIPASA can solve a similar, simplified problem. If the stiffened panel is replaced by an equivalent orthotropic panel with smeared stiffnesses, the resulting panel is uniform in both directions. For this case, the panel can be

rotated 90° and boundary conditions can be modeled correctly on the edges normal to the stiffeners. The result of such an analysis would be similar to that shown in figure 22. Let the value of F for this smeared orthotropic panel be denoted $F_{s,90}$.

In the adjusted analysis approach, it is assumed that $F_{d,90}$ can be approximated by

$$F_{d,90} = \frac{F_{d,0}}{F_{s,0}} F_{s,90} \quad (45)$$

where all three values of F on the right side of the equation are calculated with VIPASA, and the models used in the analyses are illustrated in figure 23.

In equation (45), both smeared solutions are based on the orthotropic stiffnesses discussed in the section entitled Smeared Orthotropic Stiffnesses. All other stiffnesses are assumed to be zero. The quantities $F_{d,0}$ and $F_{s,0}$ are calculated for $\lambda = L$. The quantity $F_{s,90}$ is associated with the lowest of the buckling loads calculated for $\lambda = W, W/2, W/3, \dots, W/\text{MINLAM}$, where W is the panel width. Multiplying $F_{s,90}$ by the ratio of $F_{d,0}$ to $F_{s,0}$ is an attempt to remove analysis inadequacies caused by representing the discretely stiffened panel by a smeared orthotropic panel. Note that $F_{d,0}$ is the standard VIPASA solution.

The input parameter SHEAR is used to indicate whether the adjusted analysis is to be used for the $\lambda = L$ buckling load.

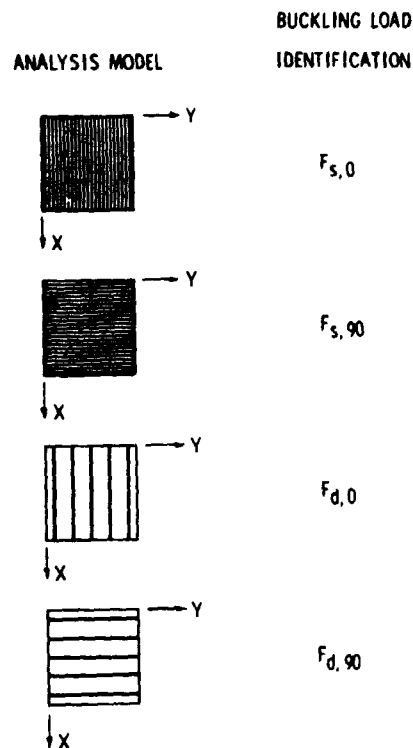


Figure 23.- Analysis models used to obtain adjusted solution for shear buckling.

If $SHEAR = 0$, the standard VIPASA analysis is used. If $SHEAR > 0$, the adjusted analysis is used. When $SHEAR > 0$, the value of the twisting stiffness used in calculating the smeared orthotropic plate buckling load is the product of $SHEAR$ and the value of the twisting stiffness calculated by equations (43) and (44). A value of $SHEAR$ less than 1 is generally appropriate for a panel composed of closed section stiffeners, such as a hat-stiffened panel.

If the adjusted analysis is selected for the $\lambda = L$ buckling load, PASCO automatically carries out the three analyses on the right side of equation (45), and chooses for the adjusted solution the smaller of the following values of F : (1) $F_{d,90}$

calculated from equation (45), and (2) $F_{s,90}$ calculated directly by VIPASA.

To summarize the various possibilities for F :

- When the adjusted shear analysis is used ($SHEAR \neq 0$ and $\lambda = L$), F is the smaller of $F_{d,90}$ and $F_{s,90}$.
- For all other cases ($SHEAR = 0$ or $\lambda \neq L$), F is $F_{d,0}$.

The appropriate value of F is then used to calculate bending loads and constraints on buckling or vibration.

The adjusted analysis is an engineering approximation, and engineering judgment should be used in its application. For example, the smeared stiffening approach must be compatible with the $F_{s,0}$ and $F_{s,90}$ buckle mode shapes. In both cases, the buckle length transverse to the stiffening must be greater than 2.5 times the stiffener spacing. If the adjusted analysis is used and if it is appreciably greater than the standard VIPASA analysis, then a factor of safety of 10 percent to 20 percent is recommended for the $\lambda = L$ buckling load. For sizing purposes, this factor of safety can be introduced with $CLAM(1) = 1.1$ or 1.2 . (See ref. 9 for additional discussion and examples.)

Example.— An example which illustrates the approach used in the adjusted shear analysis is presented in figure 24. In this figure, buckling interaction curves for shear and compression are shown for a 76.2 cm (30 in.) square, blade-stiffened panel having six stiffeners. The desired boundary conditions are simple support on all four edges, a condition that cannot be met with VIPASA if shear is present. The four curves represent the

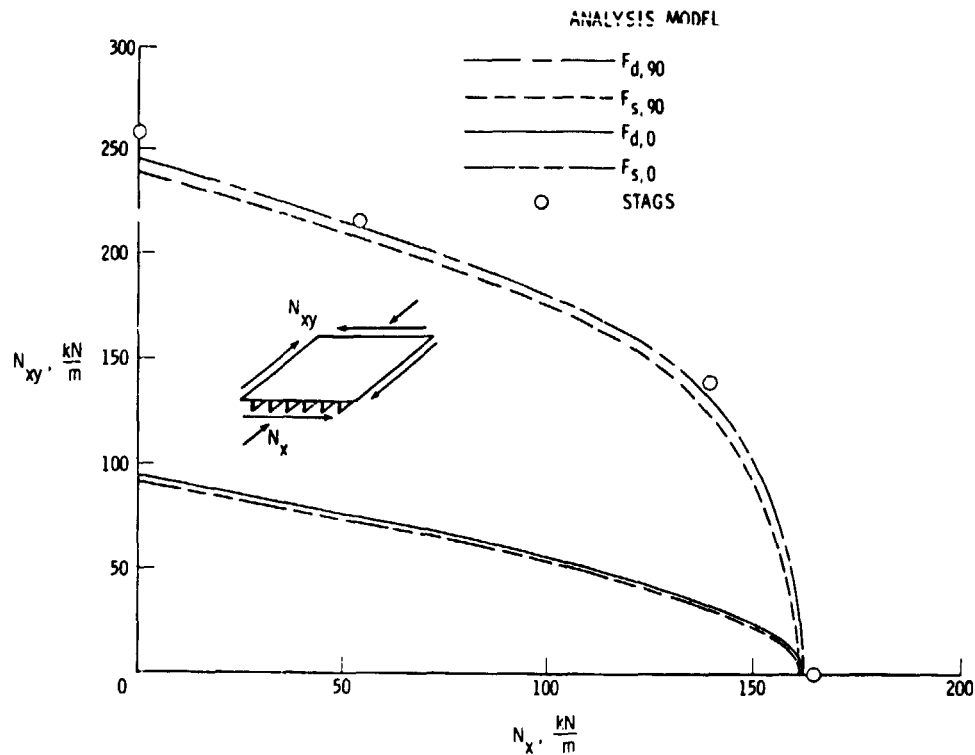


Figure 24.- Comparison of predicted buckling loads from various analysis models for blade-stiffened panel subjected to combined longitudinal compression and shear loadings.

four solution approaches just discussed and are identified in the figure key. In particular, the solid curve represents the standard VIPASA analysis, and the highest curve represents the solution obtained using equation (45). The circular symbols indicate results obtained with the STAGS computer program (ref. 10). In the STAGS analysis, the panel was modeled in detail with discrete stiffeners, and the desired simple support boundary conditions were maintained on all four edges. For this problem, the standard VIPASA analysis greatly underestimates the shear buckling load. Either of the two upper curves provides a reasonably accurate estimate of the correct result obtained with

the general two-dimensional STAGS analysis. As explained earlier, if an adjusted analysis were desired, PASCO would automatically choose the lower of the two upper curves. (See examples, ref. 9.)

SIZING

The computerized structural sizing approach used in PASCO is based on nonlinear mathematical programming techniques. Sizing variables are automatically adjusted to obtain a design that minimizes an objective function subject to a set of inequality constraints. Approximate analysis techniques are used to improve computational efficiency.

Problem Statement

The general problem statement is: find values for the set of variables X_i to

- Minimize an objective function $OBJ(X_i)$
- Subject to
 - Behavioral constraints: $G_j(X_i) \leq 0$
 - Side constraints: $VLB_i \leq X_i \leq VUB_i$

where

X_i are the sizing variables

VLB_i are the lower bounds on the sizing variables

VUB_i are the upper bounds on the sizing variables

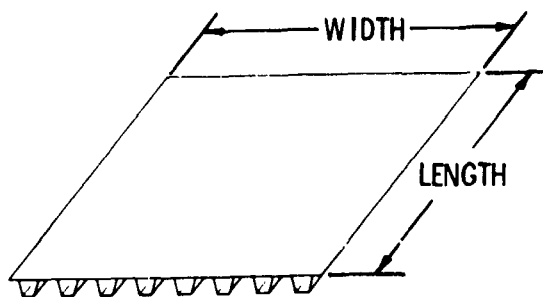
VIPASA and other analyses are used to evaluate the constraints G_j . CONMIN (refs. 11 and 12) is used to solve the resulting mathematical programming problem.

Sizing Variables

In PASCO, the sizing variables are the plate element widths, denoted b , the ply thicknesses, denoted t , and the ply orientation angles, denoted θ . Any set of widths, thicknesses, and orientation angles can be selected as the active sizing variables. The remaining widths, thicknesses, and orientation angles can be held fixed or linked linearly to the active sizing variables. Upper and lower bounds can be specified for the sizing variables.

Objective Function

The objective function is the panel mass index $\frac{W/A}{L}$, the panel mass per unit area divided by the panel length. This is the quantity denoted OBJ in CONMIN. The area A is the panel planform area shown in figure 25. Since the panel length L is fixed, the quantity that is minimized becomes the panel mass per unit width.



$$A = \text{LENGTH} \cdot \text{WIDTH}$$

Figure 25.- Panel planform area A .

Constraints

Constraints are inequality requirements that must be met during sizing to provide an acceptable design. In addition to upper and lower bounds on the sizing variables, denoted side constraints, there are behavioral constraints on buckling, material strength, stiffness, and vibration frequency. CONMIN requires that these constraints be written in the form

$$G_j \leq 0 \quad (46)$$

In PASCO, the constraints are normalized in order that all constraints be of the same order of magnitude. The specific forms for the constraints are given in the following sections.

Buckling or vibration.- Constraints on the buckling load or vibration frequency can be written in the form

$$G = 1 - \frac{F(\lambda_j)}{CLAM(\lambda_j)} \quad (47)$$

in which F is defined in equation (39), and CLAM can be used to specify a margin of safety at specific wavelengths. There can be simultaneous buckling or frequency constraints for many values of λ , and there can be many buckling or frequency constraints for each value of λ .

In the coding within PASCO, F is replaced by $N_{x_{cr}}/N_{x_{input}}$, which is equivalent to F . If the adjusted shear analysis is

selected, the appropriate analysis is used to compute $N_{x_{cr}}$. If $N_{x_{input}}$ is zero, a small positive value of $N_{x_{input}}$ is automatically introduced within PASCO.

Material strength.- Three material strength criteria are built into PASCO: maximum lamina stress, maximum lamina mechanical strain, and Tsai-Wu (ref. 13). In the maximum stress criterion, tension and compression limits are placed on σ_1 , σ_2 , and τ_{12} in each lamir . The maximum lamina mechanical strain criterion is defined similarly, except that the thermal strain is subtracted from the total strain to provide the mechanical strain in each element. For the maximum lamina stress and maximum lamina mechanical strain criteria, the material strength constraint is written in the form

$$G = \frac{S}{S_{allow}} - 1 \quad (48)$$

in which S is a lamina stress or mechanical strain, and S_{allow} is the corresponding maximum allowable value. The input quantity ALLOW is used to prescribe the allowable values used in the material strength criteria.

In the Tsai-Wu criterion, the stress state is defined by

$$\begin{aligned} \phi = & F_1\sigma_1 + F_2\sigma_2 + F_{11}\sigma_1^2 + F_{22}\sigma_2^2 \\ & + F_{66}\tau_{12}^2 + 2F_{12}\sigma_1\sigma_2 \end{aligned} \quad (49)$$

where F_1 , F_2 , F_{11} , F_{22} , and F_{66} are automatically calculated from the allowable stresses that are included in the input ALLOW, and F_{12} is included in the input ALLOW. The Tsai-Wu strength constraint is defined as

$$G = \phi - 1 \quad (50)$$

The user may incorporate his own material strength criteria by writing additional subroutines.

Stiffness.- Stiffness constraints are written as

$$G = 1 - \frac{\text{Stiffness}}{\text{Stiffness lower limit}} \quad (51)$$

and

$$G = \frac{\text{Stiffness}}{\text{Stiffness upper limit}} - 1 \quad (52)$$

in which the stiffnesses that can be constrained are:

- A_{11} extensional stiffness
- A_{33} shear stiffness
- D_{11} bending stiffness

These stiffnesses are "smeared" orthotropic stiffnesses for the overall panel, not individual plate element stiffnesses.

Approximate Analysis

The approximate analysis approach used in PASCO is depicted in figure 26. It is similar to the approach proposed in reference 14. The procedure consists, conceptually, of three modules: an analysis module, a Taylor series module, and a sizing module.

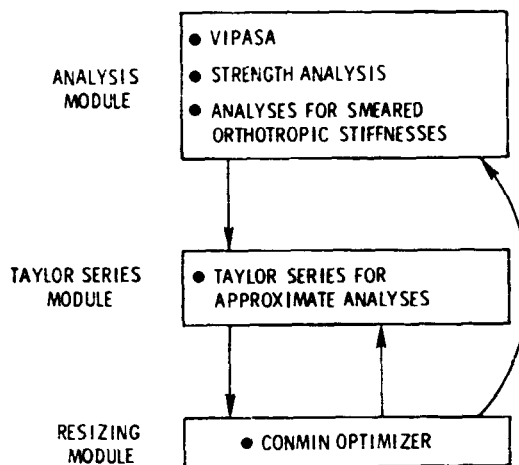


Figure 26.- General approach used in PASCO.

Analysis module.- In the analysis module, all constraints are calculated with VIPASA and supporting subroutines. The program identifies the critical constraints and, using a two-point forward difference approximation, calculates the derivatives of the critical constraints with respect to the sizing variables. The values of the constraints and derivatives are then passed to the second module, the Taylor series module. The techniques used to identify critical constraints are discussed subsequently.

Taylor series module.- The Taylor series module generates a first order Taylor series expansion of each constraint. Expansions are of the form

$$G(X_i) = G(\bar{X}_i) + \sum_i (X_i - \bar{X}_i) \left(\frac{\partial G}{\partial X_i} \right)_{X_i = \bar{X}_i} \quad (53)$$

in which X_i are the sizing variables and \bar{X}_i are the values of the sizing variables at the initial point of the expansion. The Taylor series approximations provide a reasonably accurate and simple representation of the constraints in the neighborhood of the initial point of the expansion. The Taylor series expansions are updated periodically to insure their adequacy. The second module also evaluates the objective function.

Sizing module.- The third module contains the optimizer CONMIN. During sizing, the optimizer interacts only with the second module which contains approximate, explicit functions for the constraints and a simple expression for the objective function. Such an approach greatly improves computational efficiency.

Sizing strategy.- The overall sizing strategy is depicted in more detail in figure 27. The strategy consists of a series of sizing cycles in which the optimizer adjusts the values of the sizing variables based on approximate values of the constraints (eq. (53)). An upper limit is imposed on the change of each sizing variable during each sizing cycle to insure the adequacy of both the list of constraints that are considered to be critical and the Taylor series expansions of those constraints. These limits to the changes in the sizing variables, referred to as

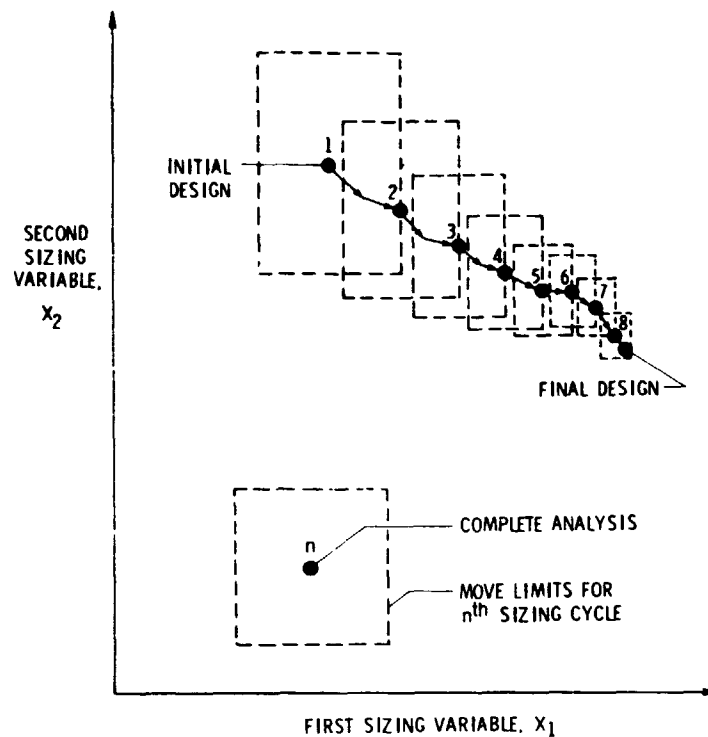


Figure 27.- Sizing strategy for approximate analysis, shown in two-sizing-variable space.

move limits, are governed by input and are indicated by the dashed rectangles in figure 27. (Move limits are discussed in the next section.) The solid circular symbol at the center of each rectangle in figure 27 represents the point at which the Taylor series expansions are carried out for each sizing cycle. The end point of one sizing cycle becomes the initial point of the next sizing cycle. Accurate values of the constraints and derivatives of the constraints are then recalculated, and new Taylor series expansions are generated. Ten sizing cycles are usually adequate to obtain convergence if the initial design is reasonably well chosen. The number of sizing cycles is controlled by the input parameter MAXJJJ and not by any convergence criterion.

Move limits.- The move limits that are generated internally for each sizing cycle are given by

$$VLB_i = \bar{X}_i - DVMOV_i \cdot (SFACTR)^{n-1} \cdot X_{i,init} \quad (54)$$

$$VUB_i = \bar{X}_i + DVMOV_i \cdot (SFACTR)^{n-1} \cdot X_{i,init} \quad (55)$$

where

- VLB_i and VUB_i are the sizing variable lower and upper bounds used by CONMIN in a sizing cycle

- \bar{X}_i are the values of the sizing variables at the beginning of a sizing cycle

- $DVMOV_i$ is an input vector
- $SFACTR$ is an input scaler
- n is the sizing cycle number

- $X_{i,init}$ are the initial (input) values of X_i

One of the objectives of equations (54) and (55) is to reduce the move limits as the sizing progresses. Overall lower and upper bounds on the sizing variables override the lower and upper bounds for a sizing cycle calculated in equations (54) and (55). Values of $DVMOV = 0.2$ and $SFACTR = 0.8$ generally provide reasonable answers.

Identifying critical buckling and frequency constraints.-

For simplicity, buckling terminology rather than eigenvalue terminology is used to describe the logic for identifying critical eigenvalue constraints for the Taylor series module. However, the discussion also applies to the frequency constraints.

The critical buckling constraints are identified by buckling half-wavelength λ . Selecting these critical values of λ is a multistep process which begins by constructing a table of potentially critical values of λ . This table always contains $\lambda = L$. The table also contains values of λ specified in the input NLAM. Also added to the table is each value of λ for which the buckling load meets both of the following two requirements.

- The buckling load is a relative minimum ($\lambda = L/8$ in figure 17), and
- The buckling load is lower than the buckling load for the preceding value of λ in the λ table. The λ table is ordered according to decreasing values of λ .

As the sizing progresses, new values of λ meeting these two requirements are identified and added to the table.

Buckling constraints are retained for a maximum of MAXL values of λ , in which MAXL is an input parameter. If there are more than MAXL values of λ in the λ table, logic is included which divides the range of m values ($m = 1, 2, 3, \dots, \text{MINLAM}$) into regions and retains the most critical constraint(s) in each region. The larger MAXL, the larger the number of regions. At this stage, $\lambda = L$ is always retained in the table of potentially critical values of λ .

The number of buckling constraints can be further reduced with the parameter GRANGE. All buckling constraints for which $F/CLAM > GRANGE$ are eliminated. For example, for $GRANGE = 2$ any buckling constraint for which G is less than -1.0 is eliminated. To insure computational efficiency, all buckling constraint elimination is based on the rough calculation of the buckling loads where the convergence criterion is CONV1. Fine calculations of the buckling loads and calculation of the derivatives of the buckling loads are not carried out for buckling constraints that are eliminated.

Identifying other critical constraints. - For constraints other than buckling, GRANGE is the sole constraint deletion mechanism. For constraints involving a lower bound (buckling, stiffness, frequency) the minimum value of G retained is

$$G = 1 - GRANGE \quad (56)$$

For constraints involving an upper bound, (stiffness, material strength) the minimum value of G retained is

$$G = \frac{1}{GRANGE} - 1 \quad (57)$$

Calculation of Derivatives of Buckling Loads

The derivatives of the buckling loads with respect to sizing variable X_i are calculated using the following numerical approximation

$$\frac{dF}{dX_i} \approx \frac{F(X_i + \Delta X_i) - F(X_i)}{\Delta X_i} \quad (58)$$

Derivatives are calculated only for those values of the half-wavelength λ identified as being critical. Two methods are available in PASCO for calculating the perturbed solution $F(X_i + \Delta X_i)$. One method uses the same general approach as that used to calculate the nominal solution $F(X_i)$. The other method uses a much faster approximate technique. The user can select the method with the input parameter JDER.

In the first method, $F(X_i + \Delta X_i)$ is calculated using an iterative technique that is the same as that used to obtain the nominal solution $F(X_i)$. The number of iterations required to obtain the perturbed solution is, however, reduced somewhat by restricting the solution for $F(X_i + \Delta X_i)$ to a narrow band centered on the nominal solution $F(X_i)$ as shown in figure 28. The solid curve indicates the value of the buckling determinant as a function of F for the nominal case. The dashed curve gives the same information for the perturbed case. The nominal solution, the band width, and the perturbed solution are indicated in the figure.

In the second method, the perturbed solution $F(X_i + \Delta X_i)$ is estimated using an approximate technique illustrated in

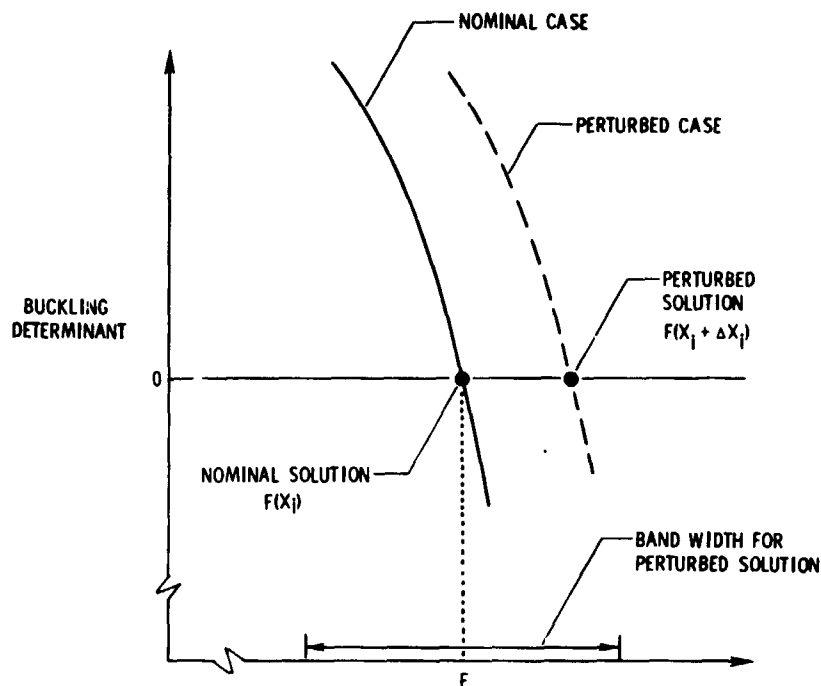


Figure 28.- Buckling determinant as a function of F for nominal values of the sizing variables and for a perturbed sizing variable.

figure 29. The approximate method³ consists of the following steps:

- Using the value of F obtained from the nominal solution shown at point 1, the value of the determinant is calculated for the perturbed case shown at point 2.
- The slope of the dashed curve at point 2 is assumed to be the same as the slope of the solid curve at point 1.
- The perturbed solution at point 3 is estimated using a linear approximation from point 2.

³The authors are indebted to Prof. Fred W. Williams, University of Wales, Institute of Science and Technology, for suggesting this technique.

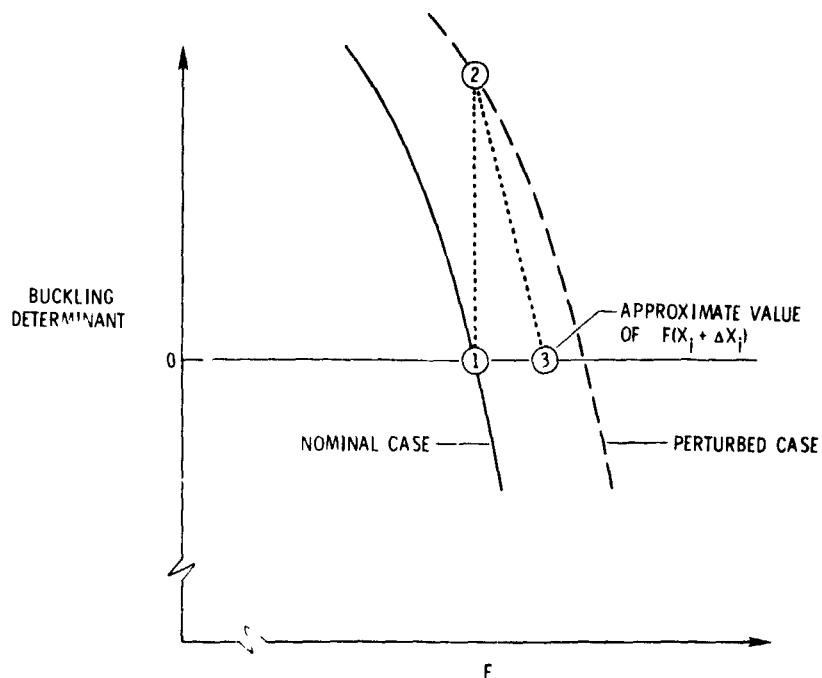


Figure 29.- Approximate method for calculating perturbed buckling load.

In all cases, the iteration scheme used to converge on an eigenvalue at point 1 involves an interval halving strategy. If certain numerical conditions are met during iteration, a linear interpolation strategy is introduced. Consider the two values of F that bracket the desired eigenvalue when the linear interpolation strategy is introduced. If these two values of F differ by at least five percent, then the second method can be used to calculate $F(X_i + \Delta X_i)$. In this case, the slope at point 1 is taken to be the last slope calculated in the linear interpolation strategy. If the numerical characteristics of the problem are such that interpolation is not used, or if, when interpolation is introduced, the two values of F that bracket

the solution differ by less than five percent, the first method is automatically used to calculate $F(X_i + \Delta X_i)$.

In the case of the adjusted analysis for shear buckling, the derivative of the adjusted buckling load for $\lambda = 1$ is taken to be

$$\frac{dF}{dX_i} = \frac{F}{F_{d,0}} \frac{d}{dX_i} F_{d,0} \quad (59)$$

where the derivative of $F_{d,0}$ is calculated using the numerical approximation in equation (58), and F is the smaller of $F_{d,90}$ and $F_{s,90}$.

Multiple Load Conditions

PASCO can treat sizing problems with multiple loading conditions. This means that panels are sized to meet the design requirements (constraints) for load condition 1 and load condition 2 and load condition 3, etc. The number of allowable load conditions is large. For limitations, see reference 1.

Using PASCO notation, quantities that can depend upon the load condition are the inplane design loads NX , NY , and NXY ; the lateral pressure $PRESS$; the bow ECC ; the change in temperature TEM ; the bending moment MX ; the design frequency $FREQ$; the material properties $E1$, $E2$, $E12$, $ANU1$, RHO , $ALFA1$, and $ALFA2$; the stiffness requirements $A11L$, $A11U$, $A33L$, $A33U$, $D11L$, and $D11U$; and the allowables $ALLOW$ used for the material strength criteria.

Sizing Example

An example which focuses on the buckling constraint aspects of the sizing code is presented in figures 30 through 32. In this example, the panel whose buckling response was shown in figure 17 is sized to meet a buckling requirement of $N_x = 700$ kN/m (4000 lbf/in). No other constraints or loadings are imposed. The panel is assumed to be perfect.

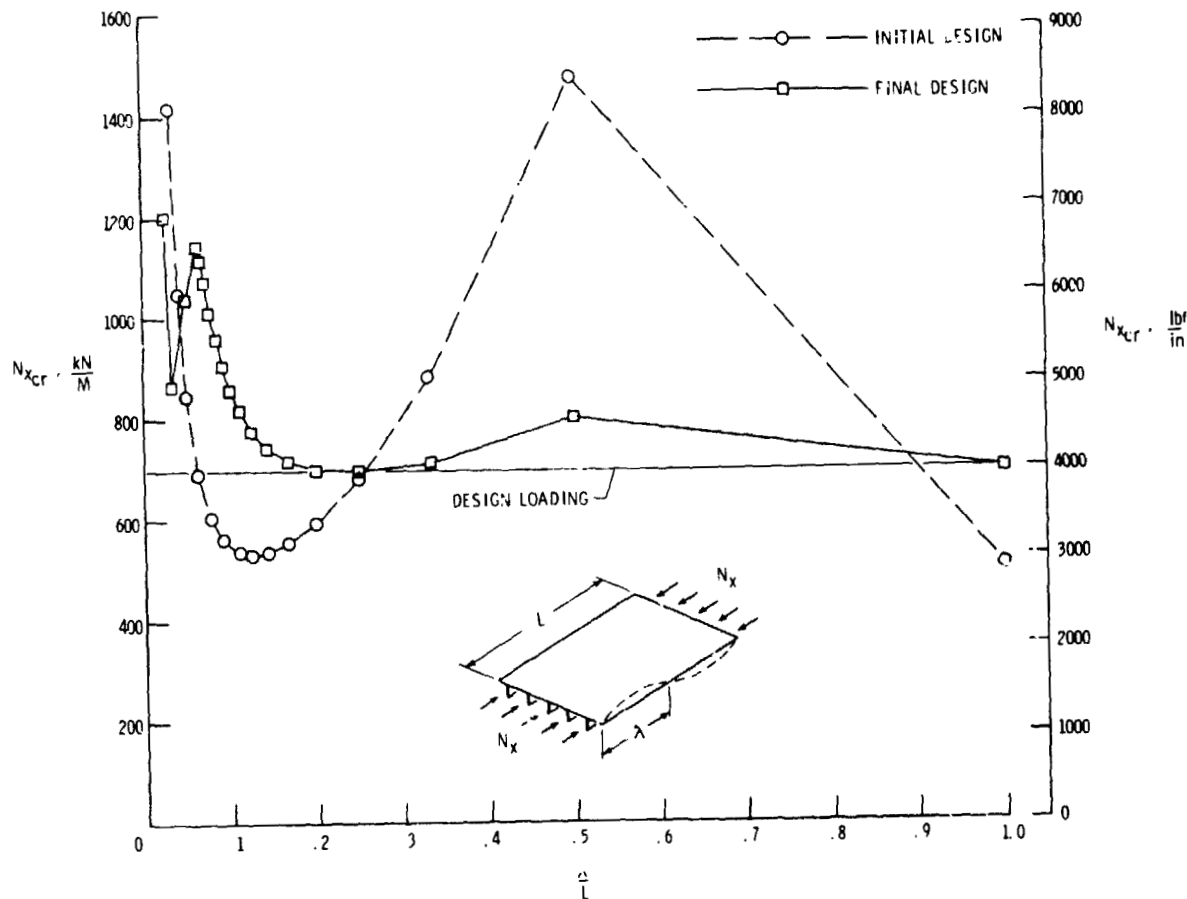


Figure 30.- Longitudinal buckling load as a function of buckling half-wavelength for two blade-stiffened panels: the initial design and the final design.

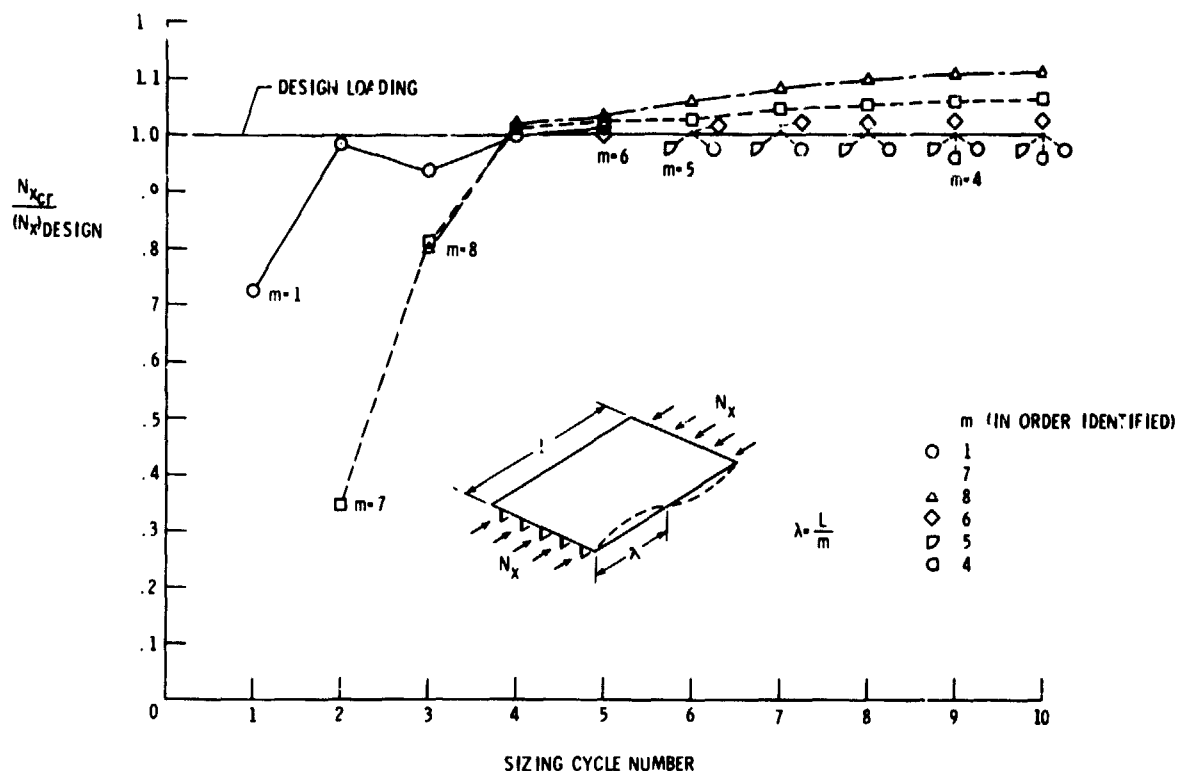


Figure 31.- Buckling loads as a function of sizing cycle number.

The buckling response for the initial design and the buckling response for the final design are both shown in figure 30. As can be seen in the figure, the initial design buckles at about 70 percent of the design load at buckling half-wavelengths of $\lambda = L$ and $\lambda = L/8$. The final design meets the buckling requirement for all values of λ .

The buckling load history for this sizing example is shown in figure 31. For the initial design, the critical buckling half-wavelength identified by the analysis module is $\lambda = L$. The half-wavelength $\lambda = L/8$ is not identified because the buckling load for $\lambda = L/8$ is slightly higher than the buckling load for $\lambda = L$. As the sizing progresses, other values of λ are

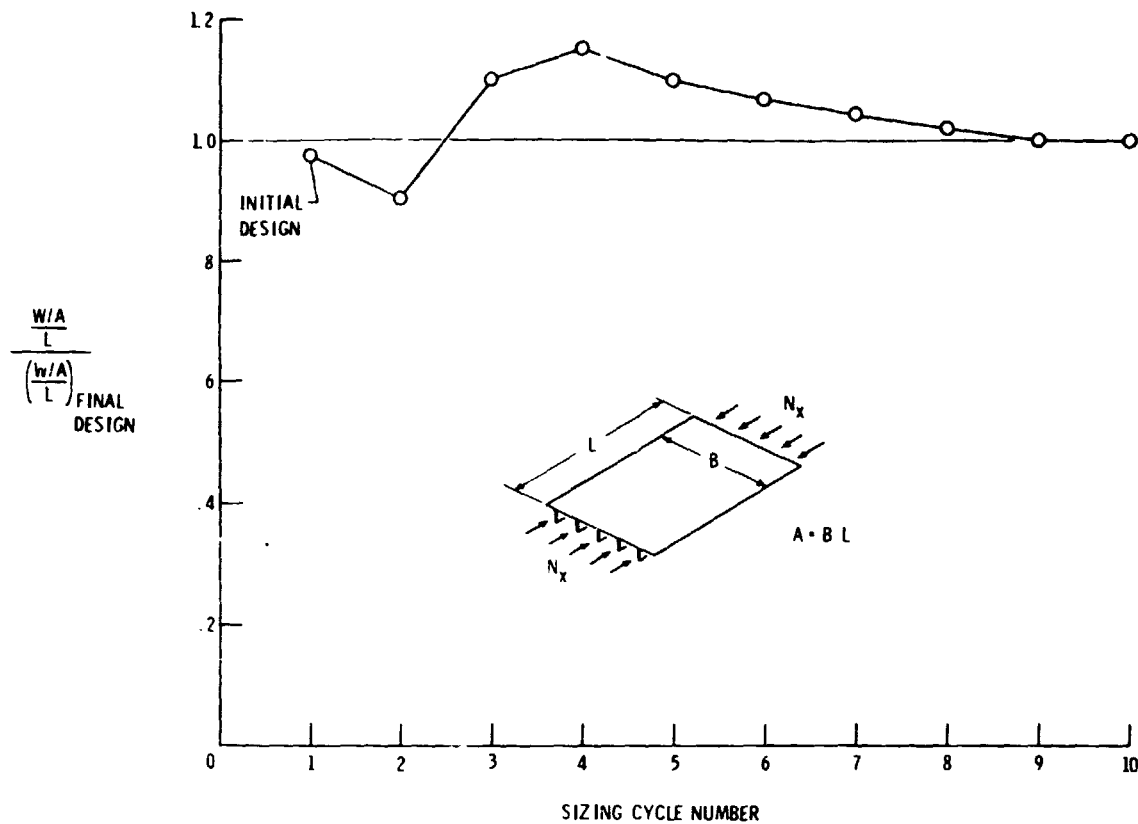


Figure 32.- Panel mass index as a function of sizing cycle number. identified and are added to the λ table. For example, at the second sizing cycle, $\lambda = L/7$ is identified, and at the third sizing cycle $L/8$ is identified.

The manner in which the mass index varies during the sizing is shown in figure 32. During the first cycle, the only buckling constraint available to PASCO was for the $\lambda = L$ mode. The code increased that buckling load while decreasing the panel mass. At the beginning of the second sizing cycle, PASCO identified the $\lambda = L/7$ mode and, during that cycle, added material to the panel to increase that buckling load. At the beginning of the fourth sizing cycle, all buckling constraints were satisfied. During

fourth and subsequent sizing cycles, the mass was reduced while the buckling strength of the panel was maintained.

In the above example, the first sizing cycle was counter-productive because the only buckling constraint available to PASCO was for the $\lambda = L$ mode. Convergence would have been improved if a local buckling constraint had been made available with the input NLAM. In this case, a good choice would have been NLAM = 7 or 8.

CONCLUDING REMARKS

This report has discussed certain aspects of the computer code denoted PASCO, which can be used for analyzing and sizing uniaxially-stiffened composite structural panels having a general configuration.

In PASCO, buckling loads, lamina stresses and strains, smeared orthotropic stiffnesses, and vibration frequencies can be calculated for a variety of typical loading conditions. These same quantities can also be used as design requirements during sizing. Sizing is based on nonlinear mathematical programming techniques in which the mass of the panel is minimized subject to satisfaction of the design requirements.

REFERENCES

1. Anderson, Melvin S.; Stroud, W. Jefferson; Durling, Barbara J.; and Hennessy, Katherine W.: PASCO: Structural Panel Analysis and Sizing Code, Users Manual. NASA TM-80182, 1981. (Supersedes NASA TM-80182, 1980.)
2. Anderson, Melvin S.; and Stroud, W. Jefferson: A General Panel Sizing Computer Code and Its Application to Composite Structural Panels. AIAA J., Vol. 17, No. 8, August 1979, pp. 892-897.
3. Williams, Jerry G.; Anderson, Melvin S.; Rhodes, Marvin D.; Starnes, James H., Jr.; and Stroud, W. Jefferson: Recent Developments in the Design, Testing, and Impact-Damage Tolerance of Stiffened Composite Panels. (Proceedings of Fourth Conference On Fibrous Composites in Structural Design), Plenum Press, 1980, pp. 259-291. Also available as NASA Technical Memorandum 80077, 1979.
4. Stroud, W. Jefferson; Agranoff, Nancy; and Anderson, Melvin S.: Minimum-Mass Design of Filamentary Composite Panels Under Combined Loads: Design Procedure Based on Rigorous Buckling Analysis. NASA TN D-8417, 1977.
5. Stroud, W. Jefferson; and Agranoff, Nancy: Minimum-Mass Design of Filamentary Composite Panels Under Combined Loads: Design Procedure Based on Simplified Buckling Equations. NASA TN D-8257, 1976.
6. Wittrick, W. H.; and Williams, F. W.: Buckling and Vibration of Anisotropic or Isotropic Plate Assemblies Under Combined Loadings. Int. J. Mech. Sci., Vol. 16, 1974, pp. 209-239.
7. Anderson, Melvin S.; Hennessy, Katherine W.; and Heard, Walter L., Jr.: Addendum to Users Guide to VIPASA (Vibration and Instability of Plate Assemblies Including Shear and Anisotropy). NASA TM X-73914, 1976.
8. Giles, Gary L.; and Anderson, Melvin S.: Effects of Eccentricities and Lateral Pressure on the Design of Stiffened Compression Panels. NASA TN D-6784, 1972.
9. Stroud, W. Jefferson; Greene, William H.; and Anderson, Melvin S.: Buckling Loads for Stiffened Panels Subjected to Combined Longitudinal Compression and Shear Loadings: Results Obtained with PASCO, EAL, and STAGS Computer Programs. NASA TM-83194, 1981.
10. Almroth, B. O.; and Brogan, F. A.: The STAGS Computer Code. NASA CR-2950, February 1978.

11. Vanderplaats, Garret N.: CONMIN - A Fortran Program for Constrained Function Minimization. User's Manual. NASA TM X-62,282, 1973.
12. Vanderplaats, G. N.; and Moses, F.: Structural Optimization by Methods of Feasible Directions. National Symposium on Computerized Structural Analysis and Design, Washington, DC, March, 1972.
13. Jones, Robert M.: Mechanics of Composite Materials. Scripta Book Co., 1975.
14. Schmit, Lucien A., Jr.; and Miura, Hirokazu: Approximation Concepts for Efficient Structural Synthesis. NASA CR-2552, 1976.